Subtype transcriptomic profiling of myeloid cells in Alzheimer Disease brain illustrates the diversity in active microglia phenotypes

Katherine E. Prater*[1] (http://orcid.org/0000-0001-8615-207X), Kevin J. Green*[1], Carole L. Smith[1], Wei Sun[2], Kenneth L. Chiou[3], Ronald Y. Kwon[4,5], Laura Heath[6], Shannon Rose[7], Ali Shojaie[8], Noah Snyder-Mackler[3], C. Dirk Keene[7], Elizabeth Blue[8,9], Jessica E. Young[5,7] Benjamin Logsdon[6,10], Gwenn A. Garden[11], and Suman Jayadev[1,5]

1 Department of Neurology, University of Washington, Seattle, WA 98195
2 Biostatistics Program, Fred Hutchinson Cancer Research Center, Seattle, WA
3 School of Life Sciences, Center for Evolution and Medicine, Arizona State University, Tempe, AZ
4 Department of Orthopaedics and Sports Medicine, University of Washington, Seattle, WA
5 Institute for Stem Cell and Regenerative Medicine, University of Washington, Seattle, WA
6 Sage Bionetworks, Seattle, WA
7 Department of Laboratory Medicine and Pathology, University of Washington, Seattle, WA
8 Department of Biostatistics, University of Washington, Seattle, WA
9 Division of Medical Genetics, University of Washington, Seattle, WA
10 Cajal Neuroscience, Seattle, WA
11 Department of Neurology, University of North Carolina, Chapel Hill, NC
* Equal co-first authors

Key words: AD, microglia, RNAseq, inflammation, human, APOE

Correspondence to:
Suman Jayadev, MD
sumie@uw.edu

Word Count:
Abstract: 230
Text: 13,701
Figures: 8
Tables: 2

Acknowledgements: Funding for these studies was provided by: RF1AG063540 and P30AG066509. Additional support was provided by the Ellison Foundation. Autopsy materials used in this study were obtained from the University of Washington Neuropathology Core, which is supported by the Alzheimer's Disease Research Center (AG05136) and the Adult Changes in Thought Study (AG006781).

Abstract:

Microglia-mediated neuroinflammation is hypothesized to contribute to disease progression in neurodegenerative diseases such as Alzheimer's Disease (AD). Microglia demonstrate heterogeneous states in health and disease, with proposed beneficial, harmful, and disease specific subtypes. Defining the spectrum of microglia phenotypes is an important step in rational design of neuroinflammation modulating therapies. To facilitate improved phenotype resolution and group comparisons based on disease state we performed single-nucleus RNA-seq on more than 120,000 microglia nuclei from AD and control dorsolateral prefrontal cortex. We identify clusters of microglia enriched for biological pathways implicating defined myeloid roles. We detected several previously unrecognized microglia populations in human AD brain, including three internalization and trafficking subtypes that were heterogeneous in their metabolic and inflammatory signatures. One of these endolysosomal subtypes is larger in AD individuals and was uniquely enriched for genes involved in nucleic acid detection and activation of interferon signaling. This inflammatory endolysosomal cluster also differentially regulated expression of genes associated with AD risk by genome wide association studies. We also identified a cluster of microglia with upregulated cell cycle and DNA repair genes that is proportionately larger in control individuals. Within cluster comparisons demonstrate that in AD brain, homeostatic microglia subpopulations upregulate inflammatory gene expression. These results highlight the heterogenous nature of the microglia response to AD pathology and will inform efforts to target specific subtypes of microglia in the development of novel AD therapies.

Introduction:

Alzheimer's Disease (AD) affects millions of individuals worldwide every year, and the projections indicate increasing impact of the disease. AD is pathologically characterized by the presence of extracellular amyloid-beta (Aβ) plaques, neuronal intracellular neurofibrillary tangles and neuroinflammation. Neuroinflammation is one hypothesized driver of the disease (Calsolaro and Edison, 2016; Salter and Stevens, 2017; Voet et al., 2019; Webers et al., 2020). Microglia are both crucial for brain function and critical elements of neuroinflammation (Streit et al., 2014; Colonna and Butovsky, 2017; Wolf et al., 2017; McQuade and Blurton-Jones, 2019; Prinz et al., 2019). In AD brain, microglia strip synapses, clear neurons by phagocytosis and release of inflammatory factors, all of which may extend and promote the pathophysiology behind cognitive decline (Jebelli et al., 2015; Colonna and Butovsky, 2017; Salter and Stevens, 2017; Hansen et al., 2018; Streit et al., 2020). As such, the dysregulated microglial inflammatory response may have potential as future therapeutic targets. Yet there remain large gaps in our understanding of the observed inflammatory behavior of microglia in AD brain.

Experimental models illustrate a wide spectrum of microglia states, though it is not yet clear which of these states or subpopulations occur and can be identified in human AD brain. While studies in human autopsy brain tissue may not currently be optimal for controlled hypothesis testing due aging effects, genomic and experiential differences within cohorts, and technical limitations, they provide unique insights into human disease pathogenesis. Defining the molecular signatures of microglial populations in human brain can give context to recognized inflammatory responses in AD (i.e. release of cytokines, dysregulated phagocytosis) as well as guide and inform hypothesis testing *in vitro* and *in vivo*.

Prior studies have identified subpopulations of microglia with specific biological function correlates in AD, and methods utilizing single cell or single nucleus RNAseq in human and

animal model brain have been critical to this effort (Keren-Shaul et al., 2017; Mathys et al., 2017, 2019; Sala Frigerio et al., 2019; Alsema et al., 2020; Nguyen et al., 2020; Olah et al., 2020; Zhou et al., 2020; Gerrits et al., 2021; Shahidehpour et al., 2021). Several studies have described a specific population of microglia in AD mouse models and AD human cases (Keren-Shaul et al., 2017; Mathys et al., 2019; Sala Frigerio et al., 2019). Termed “Disease-associated microglia” (DAMs), or alternatively activated-response microglia (ARMs), these microglia are observed in mice that express human Aβ, and microglia with similar gene expression are proportionately enriched in AD human cases. Studies in human brain autopsy tissue have identified other populations of microglia that appear to be amyloid-responsive, or have altered gene expression in the disease state (Nguyen et al., 2020; Olah et al., 2020; Gerrits et al., 2021). While informative, these studies involve relatively small numbers (100’s or perhaps 1000’s) of microglia. A recent study by Olah et al. aggregated fresh brain tissue from AD cortex and temporal lobe resection samples to profile more than 16,000 microglia revealing 9 microglia clusters (Olah et al., 2020) suggesting that larger numbers of sequenced cells will achieve finer resolution of biologically relevant subtypes.

Microglia comprise 3-8% of all cells in brain tissue (Lawson et al., 1992), therefore any single nuclei/cell sample from one brain sample in many snRNAseq approaches is limited to dozens or hundreds of cells per individual, likely limiting the identification of the breadth of microglia states actually present (Mathys et al., 2019; Nguyen et al., 2020). We posited that cellular processes upstream of the well-recognized “inflammatory” or “responsive” microglia profiles may be uncovered through improved resolution of microglia phenotypes in human brain. Our study was designed to provide both a well-defined cohort population and uniform tissue samples as well as a novel enrichment technique that enhances microglia representation in the snRNAseq dataset. We hypothesized that this combination would vastly improve microglia yield per subject and allow better characterization of the changes occurring in microglia

subpopulations in AD brain. We generated microglia transcriptional profiles from a cohort of 22 individuals with mixed APOE genotype, and then in a subset cohort of 13 individuals that were all APOE 3/3 genotype. We annotated microglia subtypes with plausible biological roles and identified transcriptional differences between AD and control in particular microglial phenotypes. In addition to homeostatic and inflammatory phenotypes described in previous studies, we uncovered microglial subtypes with distinct transcriptomic profiles which may provide additional clues into potential mechanisms related to known AD genetic risk factors and serve as a platform for hypotheses testing in future AD mechanistic studies.

Methods:

Human Brain Tissue: Prefrontal cortex (PFC) tissue from human brains was obtained from the Neuropathology Core of the Alzheimer's Disease Research Center (ADRC) at the University Washington (UW) following informed consent approved by the UW Institutional Review Board (IRB). Patients (n=12) were confirmed post-mortem to have AD according to their ADNC score of 2-3 (Table 1). Control individuals (n=10) did not meet AD diagnosis criteria post-mortem and had ADNC scores of 0-1 indicating low or no neuropathology (Table 1).

Brain samples were obtained during rapid autopsy, flash-frozen in either liquid nitrogen or isopentane and stored at -80ºC. Sample criteria for inclusion in this study included post-mortem interval (PMI) less than or equal to 10 hrs, low comorbid pathology such as Lewy Bodies and hippocampal sclerosis, and a brain pH at autopsy of six or higher (See Table S1 for additional demographic and clinical characteristics).

Isolation of Nuclei from Flash Frozen Tissue for Unsorted snRNA-seq: Nuclei from frozen rapid autopsy samples were isolated using protocols adapted from 10x Genomics Demonstrated Protocols and De Groot et al (2001). Samples were processed on ice using pre-

chilled solutions and RNAse-free instruments and equipment unless otherwise stated. Briefly, four 2mm punches of PFC gray matter were collected using a biopsy punch (Fisher Scientific, Waltham, MA) into a 1.5mL microcentrifuge tube on dry ice. Brain punches were homogenized on ice in 50µl of Nuclei Lysis Buffer (NLB: 10mM Tris-HCl pH 7.4, 10mM NaCl, 3mM $MgCl_2$, 0.1% NP-40 Alternative (Calbiochem, La Jolla, CA) 0.5% Protector RNase Inhibitor (Sigma Aldrich, St Louis, MO) and 100µM Aurintricarboxylic acid (ATA) in nuclease-free water) using a disposable pestle (USA Scientific, Ocala, FL). The pestle was rinsed into the sample tube with 900µL of NLB and the homogenate was thoroughly mixed using a regular-bore P1000 tip. The homogenate was incubated at 4ºC under gentle agitation for 10 min, pelleted at 500 x g for 7 min at 4ºC and resuspended in 500µL Nuclei Suspension Solution (NSS: phosphate buffered saline (PBS) supplemented with 100µM ATA, 1% bovine serum albumin (BSA), and 0.5% Protector RNase Inhibitor). The nuclei suspension was carefully layered onto 900µL of Percoll/Myelin Gradient Buffer (PMGB) consisting of 51% myelin gradient buffer (MGB; De Groot et al., 2001), 27% Percoll (GE Healthcare, Uppsala, Sweden), 3% 10X Hanks Balanced Salt Solution without calcium, magnesium (HBSS; Fisher Scientific), 2.5% 1.5M NaCl, 0.1% 10mM ATA in MGB, and 0.5% Protector RNase Inhibitor. The gradient was centrifuged at 950 x g for 20 min at 4°C with slow acceleration and no brake. Myelin and supernatant were aspirated and the nuclei pellet was resuspended in Resuspension Buffer (RB: PBS containing 1% BSA and 0.5% Protector RNase Inhibitor) at a concentration of 1000 nuclei/µL and proceeded immediately to single-nuclei RNA sequencing (snRNA-seq).

Isolation of Nuclei from Flash Frozen Tissue for Fluorescence-activated Nuclei Sorting (FANS): Briefly, 400-500mg of PFC was collected into a 1.5 ml microcentrifuge tube on dry ice. Brain tissue was homogenized on ice in 100µl of NLB supplemented with the following protease and phosphatase inhibitors: 1X cOmplete Mini Protease Inhibitor Cocktail (Sigma-Aldrich), 0.5% Phosphatase Inhibitor Cocktail 2 (Sigma-Aldrich) and 1mM phenylmethylsulfonyl fluoride

(PMSF; Tocris Bioscience, Ellisville, MO) using a disposable pestle (USA Scientific, Ocala, FL). The pestle was rinsed with 800 µl of NLB supplemented with protease and phosphatase inhibitors into the sample tube and the homogenate was thoroughly mixed using a regular-bore P1000 tip. The homogenate was incubated at 4ºC under gentle agitation for 10min, pelleted at 500 x g for 7 min at 4ºC and resuspended in 900µL PMGB supplemented with protease and phosphatase inhibitors. The nuclei suspension was gently overlaid with 300µL NSS supplemented with protease and phosphatase inhibitors. The gradient was centrifuged at 950 x g for 20 min at 4ºC with slow acceleration and no brake. The myelin and supernatant were aspirated and the nuclei pellet proceeded immediately to FANS.

Fluorescence Activated Nuclei Sorting (FANS): Nuclei were washed with cold FANS media (10% fetal bovine serum (FBS), 10mM HEPES, 100µM ATA, 10% 10X HBSS, 0.5% Protector RNase Inhibitor, protease and phosphatase inhibitors, and 1% saponin in nuclease-free water) and resuspended in 1mL of FANS media at a concentration of 2-2.5x10^6 nuclei/mL. Nuclei were blocked with 1% Human BD Fc Block (clone Fc1.3216, BD Biosciences, San Jose, CA) and incubated on ice for 10 min. Nuclei were labeled with either anti-PU.1-PE (clone 9G7, 1:50, Cell Signaling Technology, Danvers, MA) or IgG-PE isotype control (clone DA1E, 1:50, Cell Signaling Technology) for 4 hours on ice. Nuclei were washed three times with cold FANS media and resuspended in 250 (isotype control) or 500µL (PU.1) FANS media supplemented with 10µg/mL DAPI (Sigma-Aldrich). Nuclei were sorted using a FACSAria III Cell Sorter (BD Biosciences) equipped with a 70µM nozzle until 30,000 PU.1-positive nuclei were collected in RB. Sorted nuclei were centrifuged at 1,000 x g for 10 min at 4ºC. The nuclei pellet was resuspended in RB at a concentration of 1000 nuclei/µL and proceeded immediately to snRNA-seq.

Single Nuclei RNA-Sequencing (snRNA-seq): Single nuclei libraries were generated using the Chromium Next GEM Single Cell 3' GEM, Library and Gel Bead Kit v3 (10x Genomics,

Pleasanton, CA) according to the manufacturer's protocol. Briefly, a target capture of 10,000 nuclei were loaded onto a channel of a Chromium Next GEM Chip B (10x Genomics) to generate Gel Bead-in-Emulsions (GEMs). GEMs underwent reverse transcription to barcode RNA followed by amplification, fragmentation and 5' adaptor and sample index attachment. Gene expression libraries were sequenced on the NovaSeq 6000 platform (Illumina, San Diego, CA) using a S2 100 cycle flow cell.

Alignment and Quality Control: Gene counts were obtained by aligning reads to the hg38 genome (GRCh38-1.2.0) using CellRanger 3.0.2 software (10x Genomics). Reads mapping to precursor mRNA were included, to account for unspliced nuclear transcripts. The majority of our analysis was performed in R (R Core Team, 2020). Droplets from 22 PU.1 sorted samples were combined using Seurat v3.3 (Stuart et al., 2019). Unsorted and PU.1 sorted droplets isolated from the same 4 subjects were combined using Seurat and analyzed in the same manner. Droplets containing less than 350 UMIs, less than 350 genes, or greater than 1% mitochondrial genes were excluded from analysis. The Seurat object was split by individual sample and ambient RNA was removed from the remaining droplets using SoupX (Young and Behjati, 2020). The level of contamination was estimated using expression of mitochondrial genes, with a maximum contamination estimate set to 20%, and removed. Droplets containing multiple nuclei were scored using Scrublet software with an estimated 10% doublet rate, as determined by 10x Genomics (Wolock et al., 2019). Doublet thresholds were determined manually at a local minimum in doublet score and doublets were removed. 200,948 nuclei with an average of 1,787 genes per nucleus remained in the dataset for further analysis.

Normalization and Cell Clustering: Normalization and clustering of the nuclei were performed using Seurat v3.3 (Stuart et al., 2019). Data were normalized for read depth using Pearson residuals and mitochondrial gene content was regressed out using Seurat's SCTransform function (Hafemeister and Satija, 2019). Individual sample variability was removed

using Seurat's Anchoring and Integration functions (Stuart et al., 2019). Integration features were identified from the top 5000 genes across the samples using SelectIntegrationFeatures. The data was prepared using PrepSCTIntegration. The anchors were found using FindIntegrationAnchors with no reference sample, cca reduction, and 30 dimensions. The top 5000 variable genes were kept and used during principle component (PC) analysis using the RunPCA function in Seurat. 15 PCs were used to create a shared nearest neighbors graph with k=20 using the FindNeighbors function in Seurat. The modularity function was optimized using a resolution of 0.2 to determine clusters using the Louvain algorithm with multilevel refinement to determine broad cell-types. Dimensionality reduction of the clusters was performed using the RunUMAP function in Seurat.

Clusters were annotated for cell-type using manual evaluation for a set of known genetic markers (Bakken et al., 2018; Hodge et al., 2019; Mathys et al., 2019; Miller et al., 2020). A new Seurat object was made containing only the 127,371 microglia nuclei. Normalization, individual variability removal, integration, and shared nearest neighbors graph creation were repeated as above on the microglia nuclei. 20 PCs were chosen to account for a significant amount of the variance based on the elbow plot of the microglia dataset. Clusters were determined using the Leiden algorithm with method igraph and weights true. The appropriate clustering resolution was determined using 0.1 steps over a range of 0.1-0.8. The number of sub-clusters were chosen using the maximum number of sub-clusters for which no sub-cluster contained a majority of nuclei from one sample and where the clusters appeared to contain higher densities of nuclei. Clusters were highly conserved across analysis by Louvain, Louvain with multilevel refinement, and Leiden algorithms. Distribution of nuclei within each sub-cluster was calculated using (number of nuclei from a group within the sub-cluster)/(total number of nuclei of the sub-cluster)*100. Chi-squared statistics were performed with the 'chisq.test' function in R (R Core Team, 2020).

snRNA-seq Differential Gene Expression and Gene Set Enrichment Analyses:

Differential gene expression analysis of the sub-clusters was performed on the RNA assay of the Seurat object using the FindAllMarkers function in Seurat, with the MAST algorithm. Genes tested had expression in at least 25% of the nuclei in the cluster. Differentially expressed genes (DEGs) had an adjusted p-value less than 0.05 and a fold change greater than 1.25. Sub-cluster 1 was determined to be inactivated microglia nuclei. Differential gene expression analysis was repeated as above comparing each other cluster to cluster 1. GO, KEGG and Biocarta pathway sets, version 7.2, were downloaded from http://www.gsea-msigdb.org/gsea/downloads.jsp. Gene set enrichment analysis (GSEA) was performed using the GSEA function in ClusterProfiler (Yu et al., 2012; Wu et al., 2021) modified to use a set seed for reproducibility, using the above pathway sets. Genes were ordered according to the log fold change. Enriched pathways had an adjusted p-value less than 0.05. We considered pathways to be representative if significant results included similar genes and biological functions in at least two of the three major databases (GO, KEGG, Reactome).

Group Differential Gene Expression and Gene Set Enrichment Analyses: For each sample and sub-cluster, gene expression counts from the RNA assay of the Seurat object were combined from each cell to generate a “pseudobulk” dataset similar to (Thurman et al., 2021). Genes expressed in fewer than the number of nuclei in the smallest sub-cluster were removed. Differential gene expression analysis was performed using DESeq2. Regression model composition was determined using variance partitions and p-value histograms. We confirmed that there were no major artifacts in DEGs determined by our analysis by replicating the results utilizing an additional robust normaliziation method for zero-inflated datasets (Chen et al., 2018). DEGs had an adjusted p-value less than 0.1 and a fold change greater than 1.25. GSEA was performed as above with the genes ordered by the Wald statistic. Enriched pathways had an adjusted p-value less than 0.05. We considered pathways to be representative if significant

results included similar genes and biological functions in at least two of the three major databases (GO, KEGG, Reactome).

Trajectory and Lineage Analysis: Trajectory analysis was performed using Monocle3 (Trapnell et al., 2014; Qiu et al., 2017; Cao et al., 2019). The data were transferred to a cds object and Monocle3 "learn_graph" was run on the whole dataset. Subsequently, the cds was divided into AD individuals and control individuals, and "learn_graph" was applied to both individually. Lineage analysis was performed using Slingshot (Street et al., 2018). PCA and UMAP embeddings were extracted from the Seurat object. We applied the algorithm both with and without a defined starting point to the mixed APOE sample dataset.

Visualizations: Visualizations were generated using ggplot2 (Wickham et al., 2016), pheatmap, and Seurat native functionality (Stuart et al., 2019).

Results:

Fluorescence-activated nuclei sorting (FANS) for PU.1 expression enriches microglia nuclei by 20 fold. We hypothesized that much larger numbers of microglia nuclei could be evaluated by snRNAseq if fluorescence-activated nuclei sorting (FANS) for expression of a myeloid specific transcription factor (PU.1) was utilized prior to 10X Chromium snRNAseq preparation and sequencing (Figure 1A). To confirm that the PU.1 FANS approach was effective in improving myeloid cell yield, we isolated and sequenced nuclei from four individuals with and without the PU.1 FANS technique applied. We analyzed similar numbers of total nuclei in the unsorted (46,085; Figure 1B) and PU.1 sorted (41,488; Figure 1C) datasets of the four individuals (p = 0.62). The PU.1 sorted dataset contained significantly more microglia nuclei defined by high expression of *C3*, *CD74*, *C1QB*, *CX3CR1*, and *SPI1* (23,310 microglia nuclei) than the unsorted dataset (1,032 microglia nuclei), a more than 20X increase (Figure 1B,C). The

increase in microglia nuclei observed in the PU.1 sorted dataset also appears to demonstrate more complexity of microglia subclusters. We next applied PU.1 FANS to a larger cohort of 22 individuals to obtain samples highly enriched for microglia nuclei, allowing us to distinguish subclusters/subpopulations with better resolution and define their biological functions. After PU.1 FANS samples retain a variety of non-myeloid cell types after (Figure 2A). However, six individual clusters clearly demonstrate microglia gene expression, and 63% of the nuclei are identified as microglia (Figure 2B).

Complexity of microglia subpopulations. The initial dataset consisted of 205,226 nuclei. After QC including doublet removal, we identified 200,948 quality sequenced nuclei. Of those, 127,371 were microglia, with a minimum of 1,300 and an average of over 5,000 nuclei per individual. We identified 10 unique clusters, or subpopulations, of microglia (Figure 3A). Clusters were defined by assessing DEGs comparing the cluster to all other nuclei (Figure 3B). Each cluster needed to meet a minimum threshold of 30 DEGs that defined it, and we confirmed that clusters were not comprised primarily of nuclei from fewer than three individuals. These 10 subpopulations also have separable biological function correlates highlighted by the representative GO term of a pathway seen in multiple ontology database results (Figure 3C).

We identified cluster 1, the largest cluster, as the unactivated or “homeostatic” cluster based on its high expression of *CX3CR1* and *P2RY12* among other genes annotated as homeostatic (Keren-Shaul et al., 2017; Mathys et al., 2019; Nguyen et al., 2020; Gerrits et al., 2021). When compared with genes defining the homeostatic cluster in Gerrits et al. (2021), the largest microglia-specific snRNAseq study to-date, our cluster 1 matched 69% of the genes in their list. Cluster 1 also contained genes identified as “homeostatic” from two other snRNAseq publications (Keren-Shaul et al., 2017; Nguyen et al., 2020), suggesting consistency across several datasets. We defined cluster 1 as a “homeostatic” cluster now referred to as HC1. Cluster 2, while very similar to HC1 in terms of a non-activated state, was also defined by a set

of downregulated genes that differed from cluster 1 (Figure 3B). The genes downregulated in cluster 2 are largely known to be involved in inflammatory processes and include *SPP1*, *HIF1A*, *CD14*, and *MALAT1* (Keren-Shaul et al., 2017; Fujikura et al., 2019; Sala Frigerio et al., 2019; Thrupp et al., 2020). Although different in their gene expression, clusters 1 and 2 may have similar biological function.

Cluster 3 was defined from all other nuclei by a set of genes including *CD163*, *DPYD*, *FMN1*, *MERTK*, and *APOE*, all of which have been identified in human microglia subpopulations and are implicated in aggregate protein internalization (Figure 3B; Keren-Shaul et al., 2017; Mathys et al., 2019; Sala Frigerio et al., 2019; Nguyen et al., 2020; Rexach et al., 2020; Gerrits et al., 2021). These same genes define cluster 3 when DEGs were generated in comparison to HC1. Additional genes of interest suggesting biological function included *FCER1G*, *SQSTM1*, *DENND4c*, *ATG7* and *ATG16L2* involved in phagocytosis, vesicle mediated transport, and autophagy (Deng et al., 2019). The pathways enriched in cluster 3 when compared to HC1 include a variety of endosome and lysosome pathways as well as catabolism and lipid binding but few inflammatory processes. These genes and pathways suggest this cluster is internalizing and processing cargo without acquiring an inflammatory phenotype. Consistent with the characterization of this subpopulation as not inflammatory, genes involved in glycolysis such as *HK2* and *PFKFB3* are downregulated in cluster 3, suggesting these cells have not undergone a metabolic switch to glycolysis, observed in the microglia inflammatory state (Lauro and Limatola, 2020).

We identified two metabolically active clusters with distinct inflammatory characteristics. Cluster 5 was differentiated from other microglia nuclei by differential expression of *HSP90AA1, HSPH1, SRGN, HIF1A*, and *CD83* genes in addition to other heat shock protein (HSP) genes (Figure 3B). The large number of HSPs seen in the DEGs suggests that these cells are responding to external stress. Cluster 5 upregulated genes driving glycolysis including *PFKFB*3

and *HK2* when compared to HC1. These, along with enrichment of pathways of pyruvate metabolism together suggest a switch from oxidative phosphorylation to glycolysis in these cells (Lauro and Limatola, 2020). The pathways enriched in this cluster indicate it is active in endocytosis, autophagy, mitophagy (Figure 3C). The cluster 5 phenotype has not been distinguished as a subtype in prior human brain studies and is represented by stress response and autophagy.

Cluster 6 was also metabolically active, but unlike cluster 5 appears to have a more inflammatory profile. Top genes defining cluster 6 from all other nuclei by differential expression included inflammatory mediators *MEG3*, *PTGDS*, *HSPA1A*, *GAS6* (a TYRO3, AXL, MERTK ligand with anti-inflammatory properties (Gilchrist et al., 2020)), *TRIM22*, and *CKB*, among others (Figure 3B). These same genes defined cluster 6 when compared to HC1. The pathways enriched within cluster 6 demonstrate metabolic activity and response to stressors similar to cluster 5 (Fig 3C) with enrichment of GO terms, glucose catabolic and chaperone binding, NLR signaling and ubiquitin-like protein ligase activity. Unique to cluster 6, we found that the DNA repair genes *ATM*, and *RNASEH2B* (Reijns et al., 2012), both responsible for maintaining genome integrity, were downregulated. Cluster 6 was enriched for genes involved in double and single strand DNA/RNA intracellular recognition (an “antiviral” gene expression pattern) including *MAVS, TRIM22, DDX42, ADAR*, the lysosomal gene CLC-7, and mediators of the NLRP3 inflammasome including *CASP1, TXNIP, P2RX7,* and the pattern recognition receptor *CARD9* (Schoggins et al., 2011; Subramanian et al., 2013; Di Virgilio et al., 2017; Wang et al., 2017; Drummond et al., 2019; Li et al., 2019; Pagani et al., 2021). The downstream mediators of nucleic acid recognition and inflammasome activation include the type 1 interferons and we correspondingly found significantly higher levels of *IRF3, IRF5*, and *IRF7*, suggesting that cluster 6 microglia are activating pathogen receptor and inflammasome pathways leading to induction of interferon signaling molecules. While *IL1b* was enriched in this cluster, higher levels

of *IL1b* as well as expression of other inflammatory effector molecules such as NFkB were a feature of cluster 8.

Cluster 7 was defined from all other nuclei by upregulation of genes involved in migration and motility including *MYO1E*, *PTPRG*, and *GLDN* (Figure 3B; Paglinawan et al., 2003; Wenzel et al., 2015; Rangaraju et al., 2018; Smolders et al., 2019). Pathways enriched in cluster 7 also indicate these cells are motile, with changes to cytoskeleton and membrane that indicate movement of processes or the cell itself (Figure 3C). Microglia are known to have highly motile processes in addition to the ability to migrate toward chemoattractants, injuries, and plaques (Smolders et al., 2019). Our gene expression data does not clarify whether this particular subtype is mobile or motile. This particular subpopulation of microglia was also notable for upregulation of both *LPL* and *PPARG*, genes involved in lipid processing (Bozina et al., 2013).

Cluster 4 we will identify as the “Neurodegenerative” cluster. This cluster was defined from all other nuclei by upregulation of *FTH1* and *FTL* as well as a large number of ribosomal genes (Figure 3B), and were nearly identical to those genes that differentiated cluster 4 from HC1. A cluster of microglia with similar gene expression phenotype is consistently identified in AD brain in both mouse and human (Keren-Shaul et al., 2017; Mathys et al., 2017, 2019; Nguyen et al., 2020; Rexach et al., 2020; Gerrits et al., 2021). This cluster is enriched for pathways involved in apoptosis, response to interferon-gamma (IFNγ), and many mitochondrial and respiratory functions (Figure 3C). The expression of *FTL*, *FTH1*, and ribosomal genes are features of dystrophic microglia (Streit et al., 2004, 2020) which are thought to be specific to diseased tissue (Streit et al., 2009, 2020; Keren-Shaul et al., 2017).

Cluster 8 is defined from all other nuclei by upregulation of classic inflammatory activation genes including *TNFAIP3, NFKB1, TRAF3, RELB*, and those more recently associated with autophagy and inflammatory reactions in neurodegenerative disease including *TANK* and *SQSTM1* (Figure 3B; Deng et al., 2019; Van Damme and Robberecht, 2021).

Pathway analysis revealed this cluster was enriched in Toll-like receptor and RIG-1 mediated signaling consistent with activation of nucleic acid or DAMP recognition pathways (Figure 3C). Enriched pathways also included NFκB signaling and IFN signaling, consistent with the specific upregulated genes highlighted above (Figure 3C). The dramatic increase in genes and pathways associated with cytokine signaling and DAMPs suggests these cells are inflammatory microglia.

Finally, our dataset identified two clusters on the extreme ends of the proliferation spectrum. Cluster 9 is defined from all other nuclei by *TMEM2* and *HAMP* (Figure 3B). *HAMP* encodes the protein hepcidin. Found primarily in liver, hepcidin is one of the primary drivers of iron homeostasis in the human body (Ganz and Nemeth, 2012). Pathways enriched in this microglia subtype involve iron homeostasis, metal ion homeostasis and cytokine production while pathways that are negatively enriched include motility (Supplemental Table S2). This profile of increased iron accumulation and cytokine production paired with decreases in motility and phagocytosis defines senescent microglia (Angelova and Brown, 2018a; b, 2019). In contrast to the senescent profile of cluster 9, cluster 10 is defined from all other nuclei by upregulation of genes involved in cell cycle regulation including *BRIP1*, *CENPP*, *CENPK*, *MELK*, and DNA repair such as *HELLS* (Okada et al., 2006; Christou and Kyriacou, 2012; Mjelle et al., 2015; Fischer et al., 2016). The pathways enriched in cluster 10 confirm the upregulation of cell cycle processes and a downregulation of endosome and cytokine processing in these microglia (Figure 3C). The presence of multiple cell cycle and DNA repair genes and pathways in cluster 10 suggest that this subpopulation of microglia are undergoing proliferation or cell cycle. This cluster is intriguing due to the known proliferation of microglia in AD brain, and the controversial nature of populations that contribute to microglia proliferation (Elmore et al., 2014, 2015; Fuger et al., 2017; Tay et al., 2017; Huang et al., 2018; Prater et al., 2021).

APOE genotype does not substantially alter clustering of microglia subtypes. We asked whether there would be a detectable difference in the cluster profile of microglia if we were to focus solely on a cohort of APOE 3/3 individuals. To date, no studies have defined microglia subtypes in a population of individuals with a specific APOE genotype. Since the majority (13/22) of our sample were homozygous for the APOE 3 allele, we generated a subset of our dataset that consisted entirely of APOE 3/3 individuals (7 controls and 6 AD pathology). After renormalization and re-clustering, we identified 9 subpopulations of microglia (Figure 4A). These clusters were defined by genes similar to those that defined the clusters in the Mixed APOE genotype dataset (Figure 4B). We identified clusters where gene expression was very similar (~60% or higher) to the Mixed APOE dataset (Figure 4C). We found a homeostatic, neurodegenerative, inflammatory and endolysosomal clusters similar to those of the Mixed APOE cohort (Figure 4). We again detected metabolically active clusters in the APOE 3/3 genotype dataset, suggesting that the presence of multiple distinct metabolically active microglia subtypes is present in the human brain even when controlling for APOE genotype. There was significant overlap with a cell cycle cluster where Mixed APOE cluster 10 overlaps significantly (91.1%) with genes from APOE 3/3 cluster 8 (Figure 4C).

Genes implicated in AD risk and pathogenesis are differentially regulated in individual microglial subtypes. A number of studies in animals and humans have characterized the “Disease Associated Microglia” phenotype and we determined whether this set of genes was enriched in a particular subtype of our human microglia dataset. Utilizing GSEA, we determined whether gene sets reflecting biological pathways were enriched in specific clusters. While the majority of our clusters (with the exception of cluster 9) had enrichment of approximately 35 genes in the DAM geneset, cluster 4 demonstrated the highest adjusted *p*-values ($p < 0.001$) and the expected direction of gene expression in the enrichment analysis (Figure 5A). Cluster 6 also was enriched for a number of DAM genes in the expected

direction (Figure 5A). In the majority of cases, genes were specifically enriched in either cluster 4 or cluster 6. This suggests that, in our dataset, the DAM phenotype is split across more than one cluster with differing gene expression profiles and biological functions. This is not the first time that the DAM profile was demonstrated to be more complex in human tissue (Alsema et al., 2020; Nguyen et al., 2020).

Multiple AD GWAS identified risk SNPs are associated with genes expressed in microglia or myeloid cells (Henstridge et al., 2019; McQuade and Blurton-Jones, 2019; Van Acker et al., 2021). Utilizing a list of 46 genes in linkage with SNPs associated with altered AD risk (Lambert et al., 2013; Sleegers et al., 2015; Kunkle et al., 2019), we used GSEA to assess enrichment of this gene set within our microglia clusters. We observed significant enrichment ($p < 0.001$) of DEG associated with AD risk genes specifically in cluster 6 (Figure 5B). Altered expression of genes associated with AD risk was observed in both directions in cluster 6 microglia. *PICALM* and *SORL1* are significantly downregulated, while others including *APP*, *APOE*, and *BIN1* were significantly upregulated (all adjusted $p < 0.001$; Figure 5B). Our dataset is the first to localize AD risk gene expression to a specific subpopulation of human microglia.

Having detected enrichment of endolysosomal AD risk genes, we assessed whether related genesets representing various microglial biological processes were particularly enriched in one cluster. We utilized gene sets from KEGG or GO biological functions to determine enrichment of specific cell functions in different clusters identified in our dataset. Our GSEA analysis demonstrated strong enrichment ($p<0.001$) of endolysosomal genes *LGMN*, *CTSL*, and *CTSB*, in clusters 3, 6, and 7, and the pair of *CTSL* and *CSTB* in cluster 5 (Figure 5C). Our heatmap demonstrates strong upregulation of many of the GO endolysosomal gene set in cluster 6, with lesser levels in clusters 3 and 5, though not all are statistically significant (Figure 5C). We also confirmed upregulation of inflammatory TLR signaling in clusters 6 and 8 using the KEGG TLR geneset confirming the inflammatory activation phenotype of both subpopulations of

microglia (Figure 5D). We utilized the KEGG cell cycle geneset as well to confirm that cluster 10 is enriched for cell cycle genes significantly ($p < 0.001$) more so than other clusters (Figure 5E). These genesets provide additional verification of the biological functions attributed to these clusters utilizing genes not necessarily identified as differentially expressed in our dataset.

***The Cluster 6 microglia subtype is larger in AD subjects*.** While we did not detect a "DAM" phenotype, we did determine that cluster 6 s uniquely enriched for AD nuclei over control nuclei (corrected p=0.006; Figure 6). Cluster 6 contained 73% nuclei from AD individuals, where the predicted value for our dataset would be 60%. This AD enriched cluster has the highest differential regulation of genes related to top AD risk SNPs (Figure 5B; Lambert et al., 2013; Sleegers et al., 2015; Kunkle et al., 2019). This suggests that microglia with a an endolysosomal, metabolic and inflammatory profile are more often found in AD. These results confirm previously reported findings that the subpopulation of microglia proportionately altered in AD human brain differs from that identified in mouse models (Friedman et al., 2018; Olah et al., 2020).

The microglia subtype expressing high levels of cell cycle genes is depleted in AD brain. Although the focus of investigation is often on what is increased in AD brain relative to healthy aging, there is also a need to investigate populations that are present in healthy aging but reduced in AD brain. This is the case for the cluster differentially expressing cell cycle regulatory genes, which is larger in control brain compared to AD brain (Mixed APOE corrected p<0.001; APOE 3/3 corrected p<0.001). This is visualized as a density plot in Figure 6A where cluster 10 signal (lower portion of A) is more intense than the respective cluster in AD brain (Figure 6B). These data suggest that AD pathology includes a detectable reduction in a microglia subpopulation with enriched for cell cycle, proliferation, and DNA repair genes.

Microglia may transition between subpopulations differently in AD than control individuals. We were curious to identify potential transitions between subtypes of microglia in

our dataset, particularly as a hypothesis-generating exercise to examine which subtypes of microglia may be end state versus transition state. Using Monocle 3 (Trapnell et al., 2014; Qiu et al., 2017; Cao et al., 2019), we applied trajectory reconstruction and pseudotime analysis on the Mixed APOE dataset of 22 individuals (Figure 7A). The pseudotime analysis suggests that cluster 4 “neurodegenerative” and cluster 6 are later pseudotime potential endpoints (Supplemental Figure 1A). Cluster 5 also appears to be an endpoint though it is not significantly later in pseudotime than many of the other clusters. However, the branching structure between the other clusters (1, 2, 3, 7, 8, 9, 10) was enormously complex and difficult to interpret, as noted previously on other human datasets (Nguyen et al., 2020). We additionally applied Slingshot (Street et al., 2018) to identify lineages and attempt to identify directionality to transitions between subpopulations of microglia clusters. When we required Slingshot to use HC1 as the starting end of its lineage algorithm, it produced three lineages with end points of clusters 6, 4, and 8 and all three lineages transitioned through cluster 10 (Supplemental Figure 1B). These data suggest that there is a possibility that microglia need to pass through a proliferative state in order to reach other states of activation and inflammation. Both Monocle3 and Slingshot identified cluster 4 and cluster 6 as endpoints or later pseudotime phenotypes, suggesting consistency across algorithms for these two results. While these findings need additional replication in both *in vitro* and *in vivo* systems as well as human tissue, we find them suggestive that microglia may pass through multiple states to reach one of a set of multiple eventual endpoints.

We next assessed trajectories and lineages for AD individuals and control individuals separately, to determine whether the disease status of the brain would influence the trajectories detected in the dataset. Monocle 3 again provided complicated trajectories, but similar pseudotime outcomes for both control and AD individuals (Supplemental Figure 1C,D). The trajectory out to cluster 4 appeared to originate from a different cluster of nuclei (cluster 7 in

Control individuals – Supp. Figure 1C - versus cluster 3 in AD individuals Supp. Figure 1D), suggesting that different subpopulations may transition out to the "Neurodegenerative" end state depending on whether the individual has AD pathology. Slingshot detected differences in lineage between AD and control individuals, defining fewer lineages for controls than for AD individuals, though the ultimate endpoints of the lineages remained the same for each control or AD group of individuals. For control individuals, the endpoints were cluster 4 and cluster 6, suggesting that even in healthy aging, clusters 4 and 6 are transcriptionally defined final transition points for microglia populations. For AD individuals, clusters 4 and 6 were also endpoints, but cluster 5 was additionally included as a third lineage endpoint. Together, both Monocle and Slingshot suggest that the trajectories or lineage transitions between subpopulations of microglia differ between brains with AD pathology and those without. We propose this as hypothesis-generating material for future studies to investigate.

Homeostatic microglia differ between AD and controls. One of the challenges to identifying microglial single nuclei transcriptomic change in AD subjects is that to assay sufficient numbers of microglia for gene expression analysis, tissue from multiple individuals are pooled. Thus, the "AD signature" reflects the combined changes across a group of samples rather than examining each sample as a data point and accounting for associated individual variability. By increasing the microglia nuclei yield of each participant we were able to make powered analyses of gene expression changes between AD and controls as two cohorts each contributing 12 or 10 people, respectively. Our analysis suggested multiple genes change between AD individuals and control individuals, with a pattern suggesting that subpopulations with a homeostatic phenotype were more inflammatory in AD brain.

Comparison of HC1 from the AD cohort compared to controls revealed several immune genes associated with endoplasmic reticulum stress and the unfolded protein response which were highly upregulated in AD brain compared to control such as *HSPA5* (FC = 3.11, q=0.056),

and *EIF2AK3* (FC = 0.70, *q*=0.083; Figure 8A) (O'Connor et al., 2008; Correani et al., 2017; Ghemrawi and Khair, 2020; Gao et al., 2021). EIF2AK3, also known as PERK, is activated by virus (O'Connor et al., 2008). These genes have also been identified as influenced by or influencing the production of amyloid-beta (O'Connor et al., 2008; Correani et al., 2017), suggesting that their upregulation in AD brain is related to that pathology. *CD14* (FC = 1.67, *q*=0.055; Figure 8A) was also upregulated in AD brain in HC1, and is known to interact with TLR4 to enhance phagocytosis of amyloid-beta in addition to providing multiple activation paths including interferon stimulation (Becher et al., 1996; Fujikura et al., 2019). Together, the upregulation of these genes in AD brain within HC1 suggest a more inflammatory phenotype of even these unactivated, "homeostatic," microglia subpopulation cells.

Cluster 3, which we identified as consistent with a phagocytic but not inflammatory state also demonstrated upregulation of genes associated with inflammation including *NFKB1* (FC = 0.62, *q* = 0.052) and *ZNF143* (FC = 0.80, *q* = 0.084) and altered metabolism including *ATP13A3* (FC = 1.12, *q* = 0.078, Figure 8B) in AD brain compared to controls. NFκB signaling is part of the inflammatory activation processes of microglia (Rangaraju et al., 2018; Saddala et al., 2021), though *NFKB1* gene expression in particular may be anti-inflammatory (Cartwright et al., 2016). It could be that upregulation of *NFKB1* within cluster 3 in AD individuals is an attempt to maintain low levels of inflammation in this subpopulation, though further investigation is needed to confirm this. *ZNF143* is a transcription factor (Ye et al., 2020) induced by DNA damage (Ishiguchi et al., 2004) and was suggested to participate in the response to DNA damage. *ATP13A3* is localized primarily to recycling endosomes as well as early and late endosomes but not lysosomes in mammalian tissues (Sørensen et al., 2018) and may play a role in heavy metal and polyamine trafficking. The differential expression of these genes in AD cluster 3 suggests an upregulation of inflammatory and altered metabolic processing in AD brain in a

subpopulation of microglia that when analyzed as a pooled set from AD and control did not suggest an inflammatory phenotype.

In contrast to HC1 and cluster 3, we did not identify any genes altered in cluster 6, and the majority of genes altered in AD within cluster 8 were not associated with inflammation or stress pathways. Our dataset also confirmed that although these genes associated with inflammation and ER stress were upregulated in AD brain in HC1 and cluster 3, they were unchanged in clusters 8 (Supp. Figure 2) or 10 (data not shown). These results confirm that the changes we observed in several of our less activated subpopulations of microglia were not broad whole-dataset findings, but instead were driven by AD gene expression changes within specific microglia subpopulations.

While our APOE 3/3 genotype dataset was smaller and therefore not strongly powered to identify differences between AD and control in subpopulations of microglia, we highlight two of the preliminary findings from this analysis. First, the gene, *CADM2* was significantly upregulated in AD HC1 compared to controls (FC = 12.20, q = 0.039). SNP variants in *CADM2* have been associated with cognitive function including processing speed, executive function, and educational attainment, suggesting alterations in the function of this gene may contribute to changes in the cognitive function of AD individuals (Davies et al., 2016; Ibrahim-Verbaas et al., 2016). The other preliminary finding is that GSEA results suggest lower enrichment of TGF-beta associated signaling in APOE 3/3 genotype AD individuals in HC1. This lower enrichment of TGF-beta which is known to be critical for microglia maturation and maintaining microglia homeostasis in the CNS (Butovsky et al., 2014; Spittau et al., 2020), suggests that once again, unactivated microglia phenotypes such as subpopulation HC1 may be altered toward an inflammatory state in AD brain. While power to detect changes was limited by sample size, we view these results as relevant hypothesis-generating information for further investigation in larger APOE genotype controlled studies.

Discussion:

This study utilized a novel sorting technique to enrich our snRNAseq dataset for microglia, yielding better resolution of the diversity of microglia subpopulations and their alterations in AD brain. To our knowledge, this is the first report of using PU.1, a myeloid marker, to enrich for microglia nuclei isolated from post-mortem human brain. It is also the first report where a single subpopulation of microglia is identified that is both enriched in AD individuals and expression of AD risk genes. We identified ten distinct microglia subpopulations including previously described “homeostatic”, and “neurodegenerative” phenotypes (cluster 4) as well as novel subtypes with a range of activation phenotypes. The increased resolution obtained through microglial enrichment is illustrated when comparing the microglia dataset reported here to that described in one of the largest AD brain snRNAseq studies to date Mathys et al. (2019). Mathys et al. (2019) describe a Mic1 population, identified to be increased in AD individuals, defined by genes that are significant DEGs defining multiple clusters in our dataset. While the DEGs from the Mic1 population generally do not appear in our HC1, cluster 2 (not shown), or in cluster 10, they do appear in the majority of our “activated” clusters.

We identify several clusters in our dataset that appear to be unique and not previously described. Nguyen et al. (2020) identified two “inflammatory” clusters, their “ARMs” and a “dystrophic” cluster. We did not identify a single “ARMs” cluster, instead finding the ARM signature across multiple phenotypically similar but distinct clusters. The largest microglia-specific snRNAseq dataset to date distinguished microglia found in brain regions containing the combination of amyloid and tau pathologies versus just amyloid pathology (Gerrits et al., 2021). Genes identified in the clusters AD1 and AD2 defined by Gerrits et al. (Gerrits et al., 2021) are found throughout many (clusters 3, 4, 5, 6, 7, 8) of our defined microglia phenotype clusters,

suggesting that these phenotypes are not as distinct in our dataset and could also relate to differences between brain regions.

Diversity of metabolically active microglia phenotypes

Three clusters, 3, 5, and 6 were enriched for endocytosis, vesicle trafficking, endolysosomal, and autophagosome pathways. While seeming to share an overall similar biological function, the subpopulations represented phenotypically distinct features of metabolism and interferon signaling, giving clues to the factors driving inflammatory gene expression.

Immune cells are metabolically dynamic, modulating the switch from oxidative phosphorylation to glycolysis in response to cell stress and activation of pattern recognition receptors (O'Neill and Pearce, 2016). This metabolic reprogramming, originally described in cancer biology as the Warberg effect (Warburg et al., 1927), allows microglia faster ATP production and more nimble responses to environmental or intracellular inflammatory and stress stimuli such as TLR signaling, hypoxia, and mitochondrial dysfunction (Lauro and Limatola, 2020) and is implicated in AD pathophysiologic change (Ulland et al., 2017; Baik et al., 2019; Johnson et al., 2020). In our study, at least two clusters (5 and 6), seemed to have made the metabolic switch to glycolysis, indicated by increased expression of *HIF1α*, genes regulating glycolysis, and pathway enrichment in glucose metabolism, glycolysis, pyruvate metabolism, and ATP metabolism. Cluster 5 was enriched in mitophagy and autophagy which, if functioning appropriately, is a homeostatic mechanism during activation and aging (Van Acker et al., 2019; Kitada and Koya, 2021). In line with this interpretation, while metabolically active, the cluster 5 phenotype did not appear to be initiating a simultaneous inflammatory response in contrast to cluster 6. A recent proteomic analysis of isolated mouse microglia sorted by autofluorescence (indicating increased storage of lysosomal contents) has similarly demonstrated a novel microglia subtype distinguished by endolysosomal, autophagic and metabolic signatures (Burns

et al., 2020). Of note, the autophagic lysosomal subtype defined by this mouse study was present in healthy brain suggesting it may play a fundamental role throughout the lifespan. When comparing gene expression of IGAP AD risk genes, we found significantly increased expression of the protective *PICALM, MEF2C,* and *SORL1* genes in cluster 5 compared to cluster 6 (Figure 5B) underscoring the functional distinction between these two subtypes.

The cluster 6 subtype was distinct as proportionately larger in AD individuals, suggesting the microenvironment and stimuli contributing to this phenotype was more likely to be found in AD brain. In addition to lysosomal and vesicular function, cluster 6 was enriched for pathways characterized by chaperone protein folding, unfolded protein response, and aggrephagy. We speculate this profile implies that cluster 6 cells are initiating pathways to process accumulated protein aggregations. Another unique feature of cells in cluster 6 is the differentially higher expression of interferon response factor (IRF) genes IRF3, IRF5 and IRF7 and enrichment of inflammatory cytokine gene sets (Supp. Table 1). The interferon gene signature in AD tissue was reported by several groups (Friedman et al., 2018; Olah et al., 2020; Rexach et al., 2020) though the stimuli driving that microglia phenotype are not fully yet defined.

Roy et al. (2020) recently reported that amyloid fibrils containing nucleic acids can induce a type I interferon response and subsequent synapse loss in an animal AD model. We found the gene expression and pathway enrichment in Cluster 6 to be suggestive of a similar model of interferon signaling induction. Cluster 6 also demonstrated upregulation of genes involved in the detection of cytosolic nucleic acids. Microglia, like other myeloid cell types, have developed specialized sensors to identify invading RNA and DNA viruses (Cai et al., 2014; Song et al., 2019). These pattern associated molecular pattern (PAMP) recognition receptors, some of which localize to the endosome, recognize viral entry through the detection of cytosolic DNA, which, in a healthy cell should be confined to the nucleus. PAMP recognition receptors can also recognize self RNA and DNA released into the cytosol after lysosomal leak, nuclear

damage or, in the case of mitochondrial degradation, mitochondrial DNA (Cai et al., 2014; Wang et al., 2018; Song et al., 2019; Riley and Tait, 2020; Gauthier and Comaills, 2021). Consistent with activation of cytosolic nucleic acid recognition inflammatory pathways, genes involved in the detection of single and double strand RNA/DNA including *MAVS*, *ADAR*, and *DDX42* (Gack et al., 2007) are also differentially expressed in Cluster 6 and are known to initiate the anti-viral interferon and TLR pathways observed in Cluster 8. Aside from pathogenic release of cellular and mitochondrial nucleic acids, cells employ antiviral pattern recognition responses to prevent autonomous activation of human endogenous retroviruses (HERV; Licastro and Porcellini, 2021) which have been associated with AD tissue and pathology (Guo et al., 2018; Dembny et al., 2020). We did not assess for the presence of HERV in this study, however our results indicate evaluating for retroelements in relation to Cluster 6 microglia may provide additional insight into the possible relationship between HERV and AD pathogenesis.

Song et al. (2021) recently characterized the molecular features of cytosolic DNA in microglia, showing in their model that most cytosolic DNA was derived from the nucleus, actively transported into the cytosol, and consists primarily of AT-rich, intronic genomic sequences, rather than mitochondrial DNA. Additionally, the group demonstrated that autophagy clears cytosolic DNA and mitigates the interferon inflammatory response induced by cytosolic DNA (Song et al., 2021). In parallel, the DNA repair genes *ATM* and *RNASEH2* associated with Ataxia-Telangiectasia and the neurodevelopmental interferonopathy syndrome Aicardi-Goutières syndrome, respectively, were downregulated in Cluster 6. Both are necessary for genome integrity and loss of their function can lead to accumulation of aberrant cytosolic DNA (Pokatayev et al., 2016). Whether the observed decreased gene expression is related or contributing to the upregulation of nucleic acid sensor genes remains to be determined. These findings may frame the characterization of Cluster 6 in our study, a subtype without the robust enrichment of autophagy as cluster 5, downregulation of DNA repair genes, and upregulation of

cytosolic DNA and interferon regulatory factor gene expression. Rexach et al. (2020) leveraged informatic integration of multiple datasets including Frontotemporal Dementia (FTD) associated P301L MAPT expressing mouse model sorted microglia and human cell datasets to map the disease course trajectories of biological models in neurodegenerative disease. They found coordinated expression of NLRP3 inflammasome and nucleotide sensor antiviral pathways present in tau associated dementias, AD, FTD and Progressive Supranuclear Palsy (PSP; Rexach et al., 2020). Interestingly, AD was associated with positive regulation of the viral response while FTD and PSP tissues showed a downregulation of antiviral responses (Rexach et al., 2020). Our study in human AD tissue suggests that the detection and response to RNA/DNA is occurring in specific microglia subtypes also enriched for endolysosomal genes and pathways.

Cross talk between interferon signaling, and the inflammasome contributes to AD pathogenesis (Kopitar-Jerala, 2017) and the NLRP3 inflammasome in particular is a key component to AD neuroinflammation (Ising et al., 2019; Milner et al., 2021). The inflammatory features of cluster 6 may be consistent with activation of the NLRP3 inflammasome, which, along with mitochondrial DNA and mitochondrial ROS release, is activated by lysosome rupture and particulates (Swanson et al., 2019). *In vitro* studies to map the microglia inflammatory cascade activating NLRP3 inflammasome induced by exposure to amyloid beta and tau have demonstrated that aggregate internalization leads to lysosomal enlargement and destabilization leading to lysosome rupture, release of cathepsin B and other lysosomal contents (Halle et al., 2008; Stancu et al., 2019)

Together, clusters 3, 5, and 6 represent a diversity of endocytosis, vesicle trafficking, endolysosomal and autophagosome pathways uniquely defined within the dataset. Seminal work since the 1990s has implicated a key role of endolysosomal dysfunction in AD (Cataldo et al., 1994; Nixon and Cataldo, 1995; Funk and Kuret, 2012; Nixon, 2017). While innovative *in*

vitro and *in vivo* studies in immune cells have mapped the path from lysosomal destabilization to inflammasome activation, to date there has not yet been clear evidence from human patient tissue that these processes may occur in subpopulations of microglia. As the first to report that a specific cluster of microglia with endolysosomal function is both enriched for AD nuclei, AD risk gene expression and interferon activation, our results require further replication in other AD cohorts. Our results also suggest the need for *in vitro* studies where specific transitions between different endolysosomal phenotypes can be initiated and detected experimentally to confirm our hypotheses about the potential transitions between homeostatic endolysosomal function (clusters 3 and 5), dysfunctional endolysosomal processing (cluster 6), and inflammation (cluster 8).

Subtype-specificity of AD risk gene and endolysosomal gene expression

Multiple studies have reproducibly identified differential expression of at least 20 AD risk genes in brain from both mouse and human single cell/nucleus or bulk RNAseq studies (Rangaraju et al., 2018; Grubman et al., 2019; Pandey et al., 2019; Sala Frigerio et al., 2019; van Rooij et al., 2019; Nguyen et al., 2020; Olah et al., 2020; Rexach et al., 2020; Sierksma et al., 2020; Srinivasan et al., 2020; Gerrits et al., 2021). Several of these studies have identified expression of AD risk genes as microglia-specific (Grubman et al., 2019; Sierksma et al., 2020; Srinivasan et al., 2020). In mouse studies, AD risk genes were specifically enriched in homeostatic microglia (Rangaraju et al., 2018), activated response microglia (Sala Frigerio et al., 2019), or in M-UP3 (viral response and autophagy) microglia (Rexach et al., 2020). In human brain, several studies have previously identified AD risk genes as differentially regulated across multiple phenotypes of microglia including both homeostatic and activated subpopulations, though which risk genes were expressed differed between subpopulations of microglia (Nguyen et al., 2020; Olah et al., 2020). In one study, AD risk genes were found in just the activated microglia clusters, but were still enriched in multiple clusters (Gerrits et al., 2021).

Many of the top International Genomics of Alzheimer's Project (IGAP) genes are involved in the endolysomal system (Kunkle et al., 2019), and we found AD endolysosomal risk genes are selectively differentially regulated in cluster 6. These data support the premise that risk genes influence AD pathophysiology in the context of specific microglia phenotypes and may inform therapeutic development aimed at leveraging genomic risk to target a particular microglial response.

The endolysosomal network is critical to maintaining neural cell homeostasis and has long been implicated in AD pathogenesis. In neurons, endosomal dysfunction, indicated by enlarged early endosomes, is a defining early cytopathology of AD (Cataldo et al., 1996, 2000; Kwart et al., 2019). Subunits and interacting proteins of the multi-protein complex retromer are deficient in AD brains (Toro et al., 1990; Small et al., 2005; Dodson et al., 2006, 2008) and altering expression of these proteins lead to mis-localization of APP and increased amyloidogenic processing of APP in in vitro neuronal culture models (Young et al., 2018; Knupp et al., 2020). Given the significance of amyloid beta peptide clearance in AD by microglia, it is likely that GWAS study findings reflect not only neuronal endolysosomal dysfunction, but that of microglia (Lucin et al., 2013; Podleśny-Drabiniok et al., 2020). Impaired microglial endolysosomal function is often discussed in the context of insufficient amyloid clearance resulting in abeta deposition in brain (Nixon, 2017; Gabandé-Rodríguez et al., 2020; Podleśny-Drabiniok et al., 2020). Yet the endolysosomal system in microglia maintains a critical role in identifying and processing foreign microbes including initiation of TLR and interferon signaling (Honda et al., 2006; Schoggins et al., 2011; Van Acker et al., 2021). In this study we could discriminate lysosomal active microglia into a non-inflammatory autophagic phenotype (cluster 5) and a dysregulated inflammatory phenotype (cluster 6) finding the endolysosomal IGAP genes to be more strongly regulated in the latter.

A cluster enriched for cell cycle and DNA repair genes is larger in control brain

One premise behind subtyping myeloid cells in brain tissue is that the disease process may drive the development of a particular phenotype which could then provide additional clues to pathogenesis. Similarly, the loss of a phenotype in the disease state may suggest loss of a homeostatic, responsive, cluster that may be rational to target therapeutically. We found depletion of a cell cycle active subtype in AD compared to control. The presence of this cluster is interesting due to the conflicting reports of how microglia proliferate, though these are derived primarily from mouse brain (Elmore et al., 2014, 2015; Fuger et al., 2017; Tay et al., 2017; Huang et al., 2018; Prater et al., 2021). Cell cycle reentry was described in neurons in AD (Herrup, 2010), and proliferation of microglia was demonstrated in mouse models of AD (Gomez-Nicola and Perry, 2016; Fuger et al., 2017). Microglia proliferation at the site of amyloid or in specific brain regions such as hippocampus was reported in human Alzheimer Disease tissue (Marlatt et al., 2014), though our study does not localize cell cycling microglia to neuropathological hallmarks. Because the population of microglia expressing cell cycle genes is small, it is possible there may be local areas of higher proliferation in AD brain in response to Aβ plaque or tau, while overall there is a relative decrease in cells with the cell cycle profile in AD. Microglia population dynamics are known to play important roles in neurodegeneration and neuroinflammation (Gordleeva et al., 2020; Martin-Estebane and Gomez-Nicola, 2020; McDonough et al., 2020). The transition from proliferation to replicative senescence in microglia contributes to amyloid pathology in a mouse model (Hu et al., 2021), suggesting that loss of this proliferating population may be part of AD progression. This is also in line with data that removal of senescent microglia alleviates AD pathology and cognitive decline in mouse models (Bussian et al., 2018). Further studies are needed both to confirm our findings of a decrease of cell-cycle associated microglia in human AD and whether the decrease is due to a transition toward senescent phenotypes in AD brain.

The influence of aging and APOE genotype on microglia subpopulations

The influence of aging is unavoidable in a study with post-mortem AD and age-matched brain. Aging signatures have been described, unique to human, distinct from the activation profile from murine AD models yet sharing similarities with human AD signatures (Srinivasan et al., 2020). Genes suggestive of an "aging signature" are expressed in all clusters in this study (Olah et al., 2018) consistent with our older age cohort. The neurodegenerative cluster 4 was equally represented in both AD and control individuals, underscoring that there are shared immune changes intrinsic to aging, inflammaging, neurodegenerative processes, and additional epigenetic factors experienced by an adult human. Inflammaging, the immune changes associated with age and correlated with chronic low-grade inflammation (Franceschi et al., 2018), may not only confound interpretations of gene expression profiles attributable to AD, but may also contribute to the disease mechanisms hypothesized to drive AD. For instance, lysosomal function and ability to maintain homeostasis decreases with age (Cuervo and Dice, 2000; Ni et al., 2019), thus the interaction between common genetic risk, aging, and experience may in aggregate raise the risk of AD over time. Additional studies exploring differences between younger controls early onset familial AD where age of death is often in the 4rd to 5th decade (Jayadev et al., 2010; Wu et al., 2012; Pilotto et al., 2013) may help to explore the aging, inflammmaging, and AD specific signatures.

Similar to studies which have enumerated genotype for each sample, our AD cohort had a higher proportion of APOE 3/4 compared to the control group reflecting the availability of participant sample tissues from our brain bank. The degree of similarity between microglia subtypes when comparing the mixed APOE group and the APOE 3/3 cohort was notable, however the overall limited number of samples remains a significant caveat to drawing strong conclusions. The profile of gene expression changes observed in AD cases within unactivated microglia subpopulations altered depending on whether the analysis was performed in an APOE 3/3 or a mixed genotype. This finding on its own may not be surprising given the established

role of APOE allele in AD risk and progression as well as work suggesting mechanistic roles for APOE in AD immune pathophysiology. However, our cohort, like other single nuclei studies, is limited and thus any extrapolation of findings related to genotype are limited. Nevertheless, the results underline the importance of balancing and more preferably, selecting samples based on APOE genotype and the need for larger cohorts to allow for appropriate comparison.

Increased inflammatory gene expression in non-inflammatory microglia subpopulations in AD brain

Using a pseudobulk approach, we tested transcriptomic differences between AD and control individuals. Previous bulk RNAseq studies have identified upregulation of genes associated with inflammation in AD brain (Mills et al., 2013; Humphries et al., 2015; Friedman et al., 2018; Pandey et al., 2019; van Rooij et al., 2019; Rexach et al., 2020). While studies in mouse models have begun to differentiate different forms of inflammatory phenotypes or the timing of inflammation in AD, these have yet to be defined in human (Friedman et al., 2018; Rangaraju et al., 2018; Rexach et al., 2020). The significant advantage of our dataset is that we can identify AD-specific gene expression changes within the subpopulations of microglia defined by the snRNAseq dataset.

Cluster 1 in both Mixed APOE and APOE 3/3 cohorts were considered the non-activated or “homeostatic” based upon their increased expression of typical homeostatic markers, CX3CR1, P2RY12 and lack of inflammatory gene expression (Keren-Shaul et al., 2017; Nguyen et al., 2020; Gerrits et al., 2021). In our dataset, homeostatic nuclei from AD subjects differed from their control homeostatic counterparts. While both AD and control nuclei were equally represented in this group, the cells from AD subjects revealed a transcriptomic signature consistent with induction of inflammatory programs. It is possible that these cells may be in an “early” disease phase, initiating pathways distinct from aged controls and progressing to a more definitive inflammatory phenotype. Alternatively, they may still be maintaining important

homeostatic functions in AD subjects, though expressing inflammatory gene signatures reflective of their microenvironment. It is also possible that the "homeostatic cluster" is in fact more heterogeneous than we can resolve at this stage and that an AD specific cluster may reside within that group.

Cluster 3, was more "active" than Cluster 1, characterized as phagocytic and endocytic, however lacked the metabolic and inflammatory gene signature observed in other clusters (5 and 6) suggesting that Cluster 3 may also be maintaining appropriate homeostatic function. Similar to Cluster 1, when we compared AD and controls in this cluster, we found evidence of increased inflammatory and protein misfolding gene expression. Because the resolution of clusters is a function of gene expression, it is likely that with larger cohorts, further subtyping of cells that are differentially enriched in homeostatic genes, may be possible. Whereas previous work has needed to utilize single microglia from either AD or control to compare gene expression differences (Mathys et al., 2019), by increasing yield of cells per individual we identified the disease associated changes occurring within phenotypes.

Limitations

Like all snRNAseq studies there are limitations to our study. The samples available to study were from a mixed APOE genotype cohort. Although we analyzed a subset of all APOE 3/3 genotype individuals and identified similar subpopulations of microglia we cannot directly distinguish the impact of APOE4 in this cohort. Similarly, while sex was relatively balanced in the mixed cohort, future studies in cohorts balanced by sex and genotype together to study the interaction of sex and APOE will be informative and necessary to tailor interventions effectively. We investigated transcriptome signatures in the DLPFC, an area with pathology in late AD stages, but one of the last to be affected. Studies where multiple regions are available (e.g. Gerrits et al., 2021), or where regions of earlier pathology are present may provide different or additional information about regional profiles of microglia subpopulations. While our PU.1

sorting technique provides a unique way to heavily enrich our dataset for microglia nuclei and allows for greater depth of resolution at an individual level, it potentially selects for a specific population of microglia. There may be other subpopulations of microglia that are underrepresented or not found in our dataset because of varying levels of PU.1 expression in microglia. While this is possible, our enrichment technique provides a much stronger basis from which to investigate microglia nuclei. While one previous study has indicated that snRNAseq does not provide a full spectrum of microglia activation profiles (Thrupp et al., 2020), we demonstrate varying levels of many of the genes that were brought up as concerns. We hypothesize that the greater numbers of microglia nuclei provided by our enrichment technique allows for better capture of the spectrum of microglia phenotypes from unactivated to activated even in nuclei.

Another limitation to this study is that it was designed to capture transcriptomic profiles in microglia that resolve them into putative subtypes. While gene expression is a useful molecular tool for cellular subtyping, it does not always directly describe protein expression, localization, or activity (Koussounadis et al., 2015). Future studies to assess the correlation between gene and protein expression at a spatial level, regionally as well as in relation to neuropathological hallmarks, will provide further context to our understanding of the phenotypic heterogeneity captured here. Nevertheless, this novel work demonstrates the improved resolution that can be achieved in autopsy brain tissue revealing phenotypes recognized *in vitro* and in other inflammatory models, but previously unidentified in human AD brain. In doing so, these findings strengthen justification for hypothesis testing and tailor experimental modeling.

Conclusions

Studies in animal models have described a spectrum of microglia phenotypes, though confirming that diversity is present in human AD is complicated by the technical challenges of capturing sufficient microglia from brain. Our novel enrichment technique allowed us to identify

and assess alterations within specific subpopulations of microglia isolated from human post-mortem brain. Our identification of multiple internalization and trafficking clusters with varying metabolic and inflammatory states provides important information for further studies to replicate and investigate. The phenotype-specific alterations in both composition and gene expression in AD brain provide additional evidence that specific targeting of detrimental biological function rather than blanket approaches to therapeutic targeting of microglia will be critical moving forward.

References:

Alsema AM, Jiang Q, Kracht L, Gerrits E, Dubbelaar ML, Miedema A, Brouwer N, Hol EM, Middeldorp J, van Dijk R, Woodbury M, Wachter A, Xi S, Möller T, Biber KP, Kooistra SM, Boddeke EWGM, Eggen BJL. 2020. Profiling Microglia From Alzheimer's Disease Donors and Non-demented Elderly in Acute Human Postmortem Cortical Tissue. Front Mol Neurosci 13:134.

Angelova DM, Brown DR. 2018a. Model Senescent Microglia Induce Disease Related Changes in α-Synuclein Expression and Activity. Biomolecules 8:67.

Angelova DM, Brown DR. 2018b. Altered Processing of β-Amyloid in SH-SY5Y Cells Induced by Model Senescent Microglia. ACS Chem Neurosci 9:3137–3152.

Angelova DM, Brown DR. 2019. Microglia and the aging brain: are senescent microglia the key to neurodegeneration? Journal of Neurochemistry 151:676–688.

Baik SH, Kang S, Lee W, Choi H, Chung S, Kim J-I, Mook-Jung I. 2019. A Breakdown in Metabolic Reprogramming Causes Microglia Dysfunction in Alzheimer's Disease. Cell Metab 30:493-507.e6.

Bakken TE, Hodge RD, Miller JA, Yao Z, Nguyen TN, Aevermann B, Barkan E, Bertagnolli D, Casper T, Dee N, Garren E, Goldy J, Graybuck LT, Kroll M, Lasken RS, Lathia K, Parry S, Rimorin C, Scheuermann RH, Schork NJ, Shehata SI, Tieu M, Phillips JW, Bernard A, Smith KA, Zeng H, Lein ES, Tasic B. 2018. Single-nucleus and single-cell transcriptomes compared in matched cortical cell types. PLoS One [Internet] 13. Available from: https://www.ncbi.nlm.nih.gov/pmc/articles/PMC6306246/

Becher B, Fedorowicz V, Antel JP. 1996. Regulation of CD14 expression on human adult central nervous system-derived microglia. J Neurosci Res 45:375–381.

Bozina T, Simić I, Lovrić J, Pećin I, Jelaković B, Sertić J, Reiner Z. 2013. Effects of lipoprotein lipase and peroxisome proliferator-activated receptor-gamma gene variants on metabolic syndrome traits. Coll Antropol 37:801–808.

Burns JC, Cotleur B, Walther DM, Bajrami B, Rubino SJ, Wei R, Franchimont N, Cotman SL, Ransohoff RM, Mingueneau M. 2020. Differential accumulation of storage bodies with aging defines discrete subsets of microglia in the healthy brain. Elife 9:e57495.

Bussian TJ, Aziz A, Meyer CF, Swenson BL, van Deursen JM, Baker DJ. 2018. Clearance of senescent glial cells prevents tau-dependent pathology and cognitive decline. Nature 562:578–582.

Butovsky O, Jedrychowski MP, Moore CS, Cialic R, Lanser AJ, Gabriely G, Koeglsperger T, Dake B, Wu PM, Doykan CE, Fanek Z, Liu L, Chen Z, Rothstein JD, Ransohoff RM, Gygi SP, Antel JP, Weiner HL. 2014. Identification of a Unique TGF-β Dependent Molecular and Functional Signature in Microglia. Nat Neurosci 17:131–143.

Cai X, Chiu Y-H, Chen ZJ. 2014. The cGAS-cGAMP-STING pathway of cytosolic DNA sensing and signaling. Mol Cell 54:289–296.

Calsolaro V, Edison P. 2016. Neuroinflammation in Alzheimer's disease: Current evidence and future directions. Alzheimer's & Dementia 12:719–732.

Cao J, Spielmann M, Qiu X, Huang X, Ibrahim DM, Hill AJ, Zhang F, Mundlos S, Christiansen L, Steemers FJ, Trapnell C, Shendure J. 2019. The single cell transcriptional landscape of mammalian organogenesis. Nature 566:496–502.

Cartwright T, Perkins ND, L. Wilson C. 2016. NFKB1: a suppressor of inflammation, ageing and cancer. The FEBS Journal 283:1812–1822.

Cataldo AM, Hamilton DJ, Barnett JL, Paskevich PA, Nixon RA. 1996. Properties of the endosomal-lysosomal system in the human central nervous system: disturbances mark most neurons in populations at risk to degenerate in Alzheimer's disease. J Neurosci 16:186–199.

Cataldo AM, Hamilton DJ, Nixon RA. 1994. Lysosomal abnormalities in degenerating neurons link neuronal compromise to senile plaque development in Alzheimer disease. Brain Res 640:68–80.

Cataldo AM, Peterhoff CM, Troncoso JC, Gomez-Isla T, Hyman BT, Nixon RA. 2000. Endocytic pathway abnormalities precede amyloid beta deposition in sporadic Alzheimer's disease and Down syndrome: differential effects of APOE genotype and presenilin mutations. Am J Pathol 157:277–286.

Chen L, Reeve J, Zhang L, Huang S, Wang X, Chen J. 2018. GMPR: A robust normalization method for zero-inflated count data with application to microbiome sequencing data. PeerJ 6:e4600.

Christou CM, Kyriacou K. 2012. BRCA1 and Its Network of Interacting Partners. Biology (Basel) 2:40–63.

Colonna M, Butovsky O. 2017. Microglia Function in the Central Nervous System During Health and Neurodegeneration. Annu Rev Immunol 35:441–468.

Correani V, Di Francesco L, Mignogna G, Fabrizi C, Leone S, Giorgi A, Passeri A, Casata R, Fumagalli L, Maras B, Schininà ME. 2017. Plasma Membrane Protein Profiling in Beta-Amyloid-Treated Microglia Cell Line. PROTEOMICS 17:1600439.

Cuervo AM, Dice JF. 2000. When lysosomes get old☆. Experimental Gerontology 35:119–131.

Davies G, Marioni RE, Liewald DC, Hill WD, Hagenaars SP, Harris SE, Ritchie SJ, Luciano M, Fawns-Ritchie C, Lyall D, Cullen B, Cox SR, Hayward C, Porteous DJ, Evans J, McIntosh AM, Gallacher J, Craddock N, Pell JP, Smith DJ, Gale CR, Deary IJ. 2016. Genome-wide association study of cognitive functions and educational attainment in UK Biobank (N=112 151). Mol Psychiatry 21:758–767.

De Groot C j. a., Hulshof S, Hoozemans J j. m., Veerhuis R. 2001. Establishment of microglial cell cultures derived from postmortem human adult brain tissue: Immunophenotypical and functional characterization. Microscopy Research and Technique 54:34–39.

Dembny P, Newman AG, Singh M, Hinz M, Szczepek M, Krüger C, Adalbert R, Dzaye O, Trimbuch T, Wallach T, Kleinau G, Derkow K, Richard BC, Schipke C, Scheidereit C, Stachelscheid H, Golenbock D, Peters O, Coleman M, Heppner FL, Scheerer P, Tarabykin V, Ruprecht K, Izsvák Z,

Mayer J, Lehnardt S. 2020. Human endogenous retrovirus HERV-K(HML-2) RNA causes neurodegeneration through Toll-like receptors. JCI Insight 5:131093.

Deng Z, Lim J, Wang Q, Purtell K, Wu S, Palomo GM, Tan H, Manfredi G, Zhao Y, Peng J, Hu B, Chen S, Yue Z. 2019. ALS-FTLD-linked mutations of SQSTM1/p62 disrupt selective autophagy and NFE2L2/NRF2 anti-oxidative stress pathway. Autophagy 16:917–931.

Di Virgilio F, Dal Ben D, Sarti AC, Giuliani AL, Falzoni S. 2017. The P2X7 Receptor in Infection and Inflammation. Immunity 47:15–31.

Dodson SE, Andersen OM, Karmali V, Fritz JJ, Cheng D, Peng J, Levey AI, Willnow TE, Lah JJ. 2008. Loss of LR11/SORLA enhances early pathology in a mouse model of amyloidosis: evidence for a proximal role in Alzheimer's disease. J Neurosci 28:12877–12886.

Dodson SE, Gearing M, Lippa CF, Montine TJ, Levey AI, Lah JJ. 2006. LR11/SorLA expression is reduced in sporadic Alzheimer disease but not in familial Alzheimer disease. J Neuropathol Exp Neurol 65:866–872.

Drummond RA, Swamydas M, Oikonomou V, Zhai B, Dambuza IM, Schaefer BC, Bohrer AC, Mayer-Barber KD, Lira SA, Iwakura Y, Filler SG, Brown GD, Hube B, Naglik JR, Hohl TM, Lionakis MS. 2019. CARD9+ microglia promote antifungal immunity via IL-1β- and CXCL1-mediated neutrophil recruitment. Nat Immunol 20:559–570.

Elmore MR, Lee RJ, West BL, Green KN. 2015. Characterizing newly repopulated microglia in the adult mouse: impacts on animal behavior, cell morphology, and neuroinflammation. PLoS One 10:e0122912.

Elmore MR, Najafi AR, Koike MA, Dagher NN, Spangenberg EE, Rice RA, Kitazawa M, Matusow B, Nguyen H, West BL, Green KN. 2014. Colony-stimulating factor 1 receptor signaling is necessary for microglia viability, unmasking a microglia progenitor cell in the adult brain. Neuron 82:380–97.

Fischer M, Quaas M, Steiner L, Engeland K. 2016. The p53-p21-DREAM-CDE/CHR pathway regulates G2/M cell cycle genes. Nucleic Acids Res 44:164–174.

Franceschi C, Garagnani P, Parini P, Giuliani C, Santoro A. 2018. Inflammaging: a new immune–metabolic viewpoint for age-related diseases. Nat Rev Endocrinol 14:576–590.

Friedman BA, Srinivasan K, Ayalon G, Meilandt WJ, Lin H, Huntley MA, Cao Y, Lee S-H, Haddick PCG, Ngu H, Modrusan Z, Larson JL, Kaminker JS, van der Brug MP, Hansen DV. 2018. Diverse Brain Myeloid Expression Profiles Reveal Distinct Microglial Activation States and Aspects of Alzheimer's Disease Not Evident in Mouse Models. Cell Reports 22:832–847.

Fuger P, Hefendehl JK, Veeraraghavalu K, Wendeln AC, Schlosser C, Obermuller U, Wegenast-Braun BM, Neher JJ, Martus P, Kohsaka S, Thunemann M, Feil R, Sisodia SS, Skodras A, Jucker M. 2017. Microglia turnover with aging and in an Alzheimer's model via long-term in vivo single-cell imaging. Nat Neurosci 20:1371–1376.

Fujikura M, Iwahara N, Hisahara S, Kawamata J, Matsumura A, Yokokawa K, Saito T, Manabe T, Matsushita T, Suzuki S, Shimohama S. 2019. CD14 and Toll-Like Receptor 4 Promote Fibrillar Aβ

42 Uptake by Microglia Through A Clathrin-Mediated Pathway. Journal of Alzheimer's Disease 68:323–337.

Funk KE, Kuret J. 2012. Lysosomal fusion dysfunction as a unifying hypothesis for Alzheimer's disease pathology. Int J Alzheimers Dis 2012:752894.

Gabandé-Rodríguez E, Keane L, Capasso M. 2020. Microglial phagocytosis in aging and Alzheimer's disease. Journal of Neuroscience Research 98:284–298.

Gack MU, Shin YC, Joo C-H, Urano T, Liang C, Sun L, Takeuchi O, Akira S, Chen Z, Inoue S, Jung JU. 2007. TRIM25 RING-finger E3 ubiquitin ligase is essential for RIG-I-mediated antiviral activity. Nature 446:916–920.

Ganz T, Nemeth E. 2012. HEPCIDIN AND IRON HOMEOSTASIS. Biochim Biophys Acta 1823:1434–1443.

Gao S, Cheng Q-C, Hu Y-G, Tan Z-Z, Chen L, Liu S-W, Kang Q-Y, Wei T. 2021. LncRNA AK148321 alleviates neuroinflammation in LPS-stimulated BV2 microglial cell through regulating microRNA-1199-5p/HSPA5 axis. Life Sciences 266:118863.

Gauthier BR, Comaills V. 2021. Nuclear Envelope Integrity in Health and Disease: Consequences on Genome Instability and Inflammation. Int J Mol Sci 22:7281.

Gerrits E, Brouwer N, Kooistra SM, Woodbury ME, Vermeiren Y, Lambourne M, Mulder J, Kummer M, Möller T, Biber K, Dunnen WFA den, De Deyn PP, Eggen BJL, Boddeke EWGM. 2021. Distinct amyloid-β and tau-associated microglia profiles in Alzheimer's disease. Acta Neuropathol [Internet]. Available from: https://doi.org/10.1007/s00401-021-02263-w

Ghemrawi R, Khair M. 2020. Endoplasmic Reticulum Stress and Unfolded Protein Response in Neurodegenerative Diseases. Int J Mol Sci 21:6127.

Gilchrist SE, Goudarzi S, Hafizi S. 2020. Gas6 Inhibits Toll-Like Receptor-Mediated Inflammatory Pathways in Mouse Microglia via Axl and Mer. Front Cell Neurosci 14:576650.

Gomez-Nicola D, Perry VH. 2016. Analysis of Microglial Proliferation in Alzheimer's Disease. In: Castrillo JI, Oliver SG, editors. Systems Biology of Alzheimer's Disease. Methods in Molecular Biology. New York, NY: Springer. p 185–193. Available from: https://doi.org/10.1007/978-1-4939-2627-5_10

Gordleeva S, Kanakov O, Ivanchenko M, Zaikin A, Franceschi C. 2020. Brain aging and garbage cleaning : Modelling the role of sleep, glymphatic system, and microglia senescence in the propagation of inflammaging. Semin Immunopathol 42:647–665.

Grubman A, Chew G, Ouyang JF, Sun G, Choo XY, McLean C, Simmons RK, Buckberry S, Vargas-Landin DB, Poppe D, Pflueger J, Lister R, Rackham OJL, Petretto E, Polo JM. 2019. A single-cell atlas of entorhinal cortex from individuals with Alzheimer's disease reveals cell-type-specific gene expression regulation. Nat Neurosci 22:2087–2097.

Guo C, Jeong H-H, Hsieh Y-C, Klein H-U, Bennett DA, De Jager PL, Liu Z, Shulman JM. 2018. Tau Activates Transposable Elements in Alzheimer's Disease. Cell Rep 23:2874–2880.

Hafemeister C, Satija R. 2019. Normalization and variance stabilization of single-cell RNA-seq data using regularized negative binomial regression. Genome Biol 20:296.

Halle A, Hornung V, Petzold GC, Stewart CR, Monks BG, Reinheckel T, Fitzgerald KA, Latz E, Moore KJ, Golenbock DT. 2008. The NALP3 inflammasome is involved in the innate immune response to amyloid-beta. Nat Immunol 9:857–865.

Hansen DV, Hanson JE, Sheng M. 2018. Microglia in Alzheimer's disease. J Cell Biol 217:459–472.

Henstridge CM, Hyman BT, Spires-Jones TL. 2019. Beyond the neuron-cellular interactions early in Alzheimer disease pathogenesis. Nat Rev Neurosci 20:94–108.

Herrup K. 2010. The involvement of cell cycle events in the pathogenesis of Alzheimer's disease. Alzheimers Res Ther 2:13.

Hodge RD, Bakken TE, Miller JA, Smith KA, Barkan ER, Graybuck LT, Close JL, Long B, Johansen N, Penn O, Yao Z, Eggermont J, Hollt T, Levi BP, Shehata SI, Aevermann B, Beller A, Bertagnolli D, Brouner K, Casper T, Cobbs C, Dalley R, Dee N, Ding S-L, Ellenbogen RG, Fong O, Garren E, Goldy J, Gwinn RP, Hirschstein D, Keene CD, Keshk M, Ko AL, Lathia K, Mahfouz A, Maltzer Z, McGraw M, Nguyen TN, Nyhus J, Ojemann JG, Oldre A, Parry S, Reynolds S, Rimorin C, Shapovalova NV, Somasundaram S, Szafer A, Thomsen ER, Tieu M, Quon G, Scheuermann RH, Yuste R, Sunkin SM, Lelieveldt B, Feng D, Ng L, Bernard A, Hawrylycz M, Phillips JW, Tasic B, Zeng H, Jones AR, Koch C, Lein ES. 2019. Conserved cell types with divergent features in human versus mouse cortex. Nature 573:61–68.

Honda K, Takaoka A, Taniguchi T. 2006. Type I Inteferon Gene Induction by the Interferon Regulatory Factor Family of Transcription Factors. Immunity 25:349–360.

Hu Y, Fryatt GL, Ghorbani M, Obst J, Menassa DA, Martin-Estebane M, Muntslag TAO, Olmos-Alonso A, Guerrero-Carrasco M, Thomas D, Cragg MS, Gomez-Nicola D. 2021. Replicative senescence dictates the emergence of disease-associated microglia and contributes to Aβ pathology. Cell Rep 35:109228.

Huang Y, Xu Z, Xiong S, Sun F, Qin G, Hu G, Wang J, Zhao L, Liang YX, Wu T, Lu Z, Humayun MS, So KF, Pan Y, Li N, Yuan TF, Rao Y, Peng B. 2018. Repopulated microglia are solely derived from the proliferation of residual microglia after acute depletion. Nat Neurosci 21:530–540.

Humphries C, Kohli MA, Whitehead P, Mash DC, Pericak-Vance MA, Gilbert J. 2015. Alzheimer disease (AD) specific transcription, DNA methylation and splicing in twenty AD associated loci. Mol Cell Neurosci 67:37–45.

Ibrahim-Verbaas C, Bressler J, Debette S, Schuur M, Smith A, Bis J, Davies G, Trompet S, Smith J, Wolf C, Chibnik L, Liu Y, Vitart V, Kirin M, Petrovic K, Polasek O, Zgaga L, Fawns-Ritchie C, Hoffmann P, Karjalainen J, Lahti J, Llewellyn D, Schmidt C, Mather K, Chouraki V, Sun Q, Resnick S, Rose L, Oldmeadow C, Stewart M, Smith B, Gudnason V, Yang Q, Mirza S, Jukema J, deJager P, Harris T, Liewald D, Amin N, Coker L, Stegle O, Lopez O, Schmidt R, Teumer A, Ford I, Karbalai N, Becker J, Jonsdottir M, Au R, Fehrmann R, Herms S, Nalls M, Zhao W, Turner S, Yaffe K, Lohman K, van Swieten J, Kardia S, Knopman D, Meeks W, Heiss G, Holliday E, Schofield P, Tanaka T, Stott D, Wang J, Ridker P, Gow A, Pattie A, Starr J, Hocking L, Armstrong N, McLachlan S, Shulman J,

Pilling L, Eiriksdottir G, Scott R, Kochan N, Palotie A, Hsieh Y-C, Eriksson J, Penman A, Gottesman R, Oostra B, Yu L, DeStefano A, Beiser A, Garcia M, Rotter J, Nöthen M, Hofman A, Slagboom P, Westendorp R, Buckley B, Wolf P, Uitterlinden A, Psaty B, Grabe H, et al. 2016. GWAS for executive function and processing speed suggests involvement of the CADM2 gene. Mol Psychiatry 21:189–197.

Ishiguchi H, Izumi H, Torigoe T, Yoshida Y, Kubota H, Tsuji S, Kohno K. 2004. ZNF143 activates gene expression in response to DNA damage and binds to cisplatin-modified DNA. Int J Cancer 111:900–909.

Ising C, Venegas C, Zhang S, Scheiblich H, Schmidt SV, Vieira-Saecker A, Schwartz S, Albasset S, McManus RM, Tejera D, Griep A, Santarelli F, Brosseron F, Opitz S, Stunden J, Merten M, Kayed R, Golenbock DT, Blum D, Latz E, Buée L, Heneka MT. 2019. NLRP3 inflammasome activation drives tau pathology. Nature 575:669–673.

Jayadev S, Leverenz JB, Steinbart E, Stahl J, Klunk W, Yu C-E, Bird TD. 2010. Alzheimer's disease phenotypes and genotypes associated with mutations in presenilin 2. Brain 133:1143–1154.

Jebelli J, Su W, Hopkins S, Pocock J, Garden GA. 2015. Glia: guardians, gluttons, or guides for the maintenance of neuronal connectivity? Ann N Y Acad Sci 1351:1–10.

Johnson ECB, Dammer EB, Duong DM, Ping L, Zhou M, Yin L, Higginbotham LA, Guajardo A, White B, Troncoso JC, Thambisetty M, Montine TJ, Lee EB, Trojanowski JQ, Beach TG, Reiman EM, Haroutunian V, Wang M, Schadt E, Zhang B, Dickson DW, Ertekin-Taner N, Golde TE, Petyuk VA, De Jager PL, Bennett DA, Wingo TS, Rangaraju S, Hajjar I, Shulman JM, Lah JJ, Levey AI, Seyfried NT. 2020. Large-scale proteomic analysis of Alzheimer's disease brain and cerebrospinal fluid reveals early changes in energy metabolism associated with microglia and astrocyte activation. Nat Med 26:769–780.

Keren-Shaul H, Spinrad A, Weiner A, Matcovitch-Natan O, Dvir-Szternfeld R, Ulland TK, David E, Baruch K, Lara-Astaiso D, Toth B, Itzkovitz S, Colonna M, Schwartz M, Amit I. 2017. A Unique Microglia Type Associated with Restricting Development of Alzheimer's Disease. Cell 169:1276-1290.e17.

Kitada M, Koya D. 2021. Autophagy in metabolic disease and ageing. Nat Rev Endocrinol 17:647–661.

Knupp A, Mishra S, Martinez R, Braggin JE, Szabo M, Kinoshita C, Hailey DW, Small SA, Jayadev S, Young JE. 2020. Depletion of the AD Risk Gene SORL1 Selectively Impairs Neuronal Endosomal Traffic Independent of Amyloidogenic APP Processing. Cell Rep 31:107719.

Kopitar-Jerala N. 2017. The Role of Interferons in Inflammation and Inflammasome Activation. Front Immunol 8:873.

Koussounadis A, Langdon SP, Um IH, Harrison DJ, Smith VA. 2015. Relationship between differentially expressed mRNA and mRNA-protein correlations in a xenograft model system. Sci Rep 5:10775.

Kunkle BW, Grenier-Boley B, Sims R, Bis JC, Damotte V, Naj AC, Boland A, Vronskaya M, van der Lee SJ, Amlie-Wolf A, Bellenguez C, Frizatti A, Chouraki V, Martin ER, Sleegers K, Badarinarayan N, Jakobsdottir J, Hamilton-Nelson KL, Moreno-Grau S, Olaso R, Raybould R, Chen Y, Kuzma AB, Hiltunen M, Morgan T, Ahmad S, Vardarajan BN, Epelbaum J, Hoffmann P, Boada M, Beecham

GW, Garnier J-G, Harold D, Fitzpatrick AL, Valladares O, Moutet M-L, Gerrish A, Smith AV, Qu L, Bacq D, Denning N, Jian X, Zhao Y, Del Zompo M, Fox NC, Choi S-H, Mateo I, Hughes JT, Adams HH, Malamon J, Sanchez-Garcia F, Patel Y, Brody JA, Dombroski BA, Deniz Naranjo MC, Daniilidou M, Eiriksdottir G, Mukherjee S, Wallon D, Uphill J, Aspelund T, Cantwell LB, Garzia F, Galimberti D, Hofer E, Butkiewicz M, Fin B, Scarpini E, Sarnowski C, Bush WS, Meslage S, Kornhuber J, White CC, Song Y, Barber RC, Engelborghs S, Sordon S, Voijnovic D, Adams PM, Vandenberghe R, Mayhaus M, Adrienne Cupples L, Albert MS, De Deyn PP, Gu W, Himali JJ, Beekly D, Squassina A, Hartmann AM, Orellana A, Blacker D, Rodriguez-Rodriguez E, Lovestone S, Garcia ME, Doody RS, Munoz-Fernadez C, Sussams R, Lin H, et al. 2019. Genetic meta-analysis of diagnosed Alzheimer's disease identifies new risk loci and implicates Aβ, tau, immunity and lipid processing. Nat Genet 51:414–430.

Kwart D, Gregg A, Scheckel C, Murphy EA, Paquet D, Duffield M, Fak J, Olsen O, Darnell RB, Tessier-Lavigne M. 2019. A Large Panel of Isogenic APP and PSEN1 Mutant Human iPSC Neurons Reveals Shared Endosomal Abnormalities Mediated by APP β-CTFs, Not Aβ. Neuron 104:256-270.e5.

Lambert J-C, Ibrahim-Verbaas CA, Harold D, Naj AC, Sims R, Bellenguez C, Jun G, DeStefano AL, Bis JC, Beecham GW, Grenier-Boley B, Russo G, Thornton-Wells TA, Jones N, Smith AV, Chouraki V, Thomas C, Ikram MA, Zelenika D, Vardarajan BN, Kamatani Y, Lin C-F, Gerrish A, Schmidt H, Kunkle B, Dunstan ML, Ruiz A, Bihoreau M-T, Choi S-H, Reitz C, Pasquier F, Hollingworth P, Ramirez A, Hanon O, Fitzpatrick AL, Buxbaum JD, Campion D, Crane PK, Baldwin C, Becker T, Gudnason V, Cruchaga C, Craig D, Amin N, Berr C, Lopez OL, De Jager PL, Deramecourt V, Johnston JA, Evans D, Lovestone S, Letenneur L, Morón FJ, Rubinsztein DC, Eiriksdottir G, Sleegers K, Goate AM, Fiévet N, Huentelman MJ, Gill M, Brown K, Kamboh MI, Keller L, Barberger-Gateau P, McGuinness B, Larson EB, Green R, Myers AJ, Dufouil C, Todd S, Wallon D, Love S, Rogaeva E, Gallacher J, St George-Hyslop P, Clarimon J, Lleo A, Bayer A, Tsuang DW, Yu L, Tsolaki M, Bossù P, Spalletta G, Proitsi P, Collinge J, Sorbi S, Sanchez-Garcia F, Fox NC, Hardy J, Naranjo MCD, Bosco P, Clarke R, Brayne C, Galimberti D, Mancuso M, Matthews F, Moebus S, Mecocci P, et al. 2013. Meta-analysis of 74,046 individuals identifies 11 new susceptibility loci for Alzheimer's disease. Nat Genet 45:1452–1458.

Lauro C, Limatola C. 2020. Metabolic Reprograming of Microglia in the Regulation of the Innate Inflammatory Response. Front Immunol 11:493.

Lawson LJ, Perry VH, Gordon S. 1992. Turnover of resident microglia in the normal adult mouse brain. Neuroscience 48:405–415.

Li L, Ismael S, Nasoohi S, Sakata K, Liao F-F, McDonald MP, Ishrat T. 2019. Thioredoxin-Interacting Protein (TXNIP) Associated NLRP3 Inflammasome Activation in Human Alzheimer's Disease Brain. Journal of Alzheimer's Disease 68:255–265.

Licastro F, Porcellini E. 2021. Activation of Endogenous Retrovirus, Brain Infections and Environmental Insults in Neurodegeneration and Alzheimer's Disease. Int J Mol Sci 22:7263.

Lucin KM, O'Brien CE, Bieri G, Czirr E, Mosher KI, Abbey RJ, Mastroeni DF, Rogers J, Spencer B, Masliah E, Wyss-Coray T. 2013. Microglial beclin 1 regulates retromer trafficking and phagocytosis and is impaired in Alzheimer's disease. Neuron 79:873–886.

Marlatt MW, Bauer J, Aronica E, van Haastert ES, Hoozemans JJM, Joels M, Lucassen PJ. 2014. Proliferation in the Alzheimer Hippocampus Is due to Microglia, Not Astroglia, and Occurs at Sites of Amyloid Deposition. Neural Plast 2014:693851.

Martin-Estebane M, Gomez-Nicola D. 2020. Targeting Microglial Population Dynamics in Alzheimer's Disease: Are We Ready for a Potential Impact on Immune Function? Front Cell Neurosci 14:149.

Mathys H, Adaikkan C, Gao F, Young JZ, Manet E, Hemberg M, De Jager PL, Ransohoff RM, Regev A, Tsai L-H. 2017. Temporal Tracking of Microglia Activation in Neurodegeneration at Single-Cell Resolution. Cell Rep 21:366–380.

Mathys H, Davila-Velderrain J, Peng Z, Gao F, Mohammadi S, Young JZ, Menon M, He L, Abdurrob F, Jiang X, Martorell AJ, Ransohoff RM, Hafler BP, Bennett DA, Kellis M, Tsai L-H. 2019. Single-cell transcriptomic analysis of Alzheimer's disease. Nature 570:332–337.

McDonough A, Noor S, Lee RV, Dodge R, Strosnider JS, Shen J, Davidson S, Möller T, Garden GA, Weinstein JR. 2020. Ischemic preconditioning induces cortical microglial proliferation and a transcriptomic program of robust cell cycle activation. Glia 68:76–94.

McQuade A, Blurton-Jones M. 2019. Microglia in Alzheimer's Disease: Exploring How Genetics and Phenotype Influence Risk. Journal of Molecular Biology 431:1805–1817.

Miller JA, Gouwens NW, Tasic B, Collman F, van Velthoven CT, Bakken TE, Hawrylycz MJ, Zeng H, Lein ES, Bernard A. 2020. Common cell type nomenclature for the mammalian brain. eLife 9:e59928.

Mills JD, Nalpathamkalam T, Jacobs HIL, Janitz C, Merico D, Hu P, Janitz M. 2013. RNA-Seq analysis of the parietal cortex in Alzheimer's disease reveals alternatively spliced isoforms related to lipid metabolism. Neurosci Lett 536:90–95.

Milner MT, Maddugoda M, Götz J, Burgener SS, Schroder K. 2021. The NLRP3 inflammasome triggers sterile neuroinflammation and Alzheimer's disease. Curr Opin Immunol 68:116–124.

Mjelle R, Hegre SA, Aas PA, Slupphaug G, Drabløs F, Sætrom P, Krokan HE. 2015. Cell cycle regulation of human DNA repair and chromatin remodeling genes. DNA Repair 30:53–67.

Nguyen AT, Wang K, Hu G, Wang X, Miao Z, Azevedo JA, Suh E, Van Deerlin VM, Choi D, Roeder K, Li M, Lee EB. 2020. APOE and TREM2 regulate amyloid-responsive microglia in Alzheimer's disease. Acta Neuropathol 140:477–493.

Ni J, Wu Z, Stoka V, Meng J, Hayashi Y, Peters C, Qing H, Turk V, Nakanishi H. 2019. Increased expression and altered subcellular distribution of cathepsin B in microglia induce cognitive impairment through oxidative stress and inflammatory response in mice. Aging Cell 18:e12856.

Nixon RA. 2017. Amyloid precursor protein and endosomal-lysosomal dysfunction in Alzheimer's disease: inseparable partners in a multifactorial disease. FASEB J 31:2729–2743.

Nixon RA, Cataldo AM. 1995. The endosomal-lysosomal system of neurons: new roles. Trends Neurosci 18:489–496.

O'Connor T, Doherty-Sadleir KR, Maus E, Velliquette RA, Zhao J, Cole SL, Eimer WA, Hitt B, Bembinster LA, Lammich S, Lichtenthaler SF, Hébert SS, De Strooper B, Haass C, Bennett DA, Vassar R. 2008. Phosphorylation of the Translation Initiation Factor eIF2α Increases BACE1 Levels and Promotes Amyloidogenesis. Neuron 60:988–1009.

Okada M, Cheeseman IM, Hori T, Okawa K, McLeod IX, Yates JR, Desai A, Fukagawa T. 2006. The CENP-H–I complex is required for the efficient incorporation of newly synthesized CENP-A into centromeres. Nat Cell Biol 8:446–457.

Olah M, Menon V, Habib N, Taga MF, Ma Y, Yung CJ, Cimpean M, Khairallah A, Coronas-Samano G, Sankowski R, Grün D, Kroshilina AA, Dionne D, Sarkis RA, Cosgrove GR, Helgager J, Golden JA, Pennell PB, Prinz M, Vonsattel JPG, Teich AF, Schneider JA, Bennett DA, Regev A, Elyaman W, Bradshaw EM, De Jager PL. 2020. Single cell RNA sequencing of human microglia uncovers a subset associated with Alzheimer's disease. Nat Commun [Internet] 11. Available from: https://www.ncbi.nlm.nih.gov/pmc/articles/PMC7704703/

Olah M, Patrick E, Villani A-C, Xu J, White CC, Ryan KJ, Piehowski P, Kapasi A, Nejad P, Cimpean M, Connor S, Yung CJ, Frangieh M, McHenry A, Elyaman W, Petyuk V, Schneider JA, Bennett DA, De Jager PL, Bradshaw EM. 2018. A transcriptomic atlas of aged human microglia. Nat Commun 9:539.

O'Neill LAJ, Pearce EJ. 2016. Immunometabolism governs dendritic cell and macrophage function. J Exp Med 213:15–23.

Pagani I, Poli G, Vicenzi E. 2021. TRIM22. A Multitasking Antiviral Factor. Cells 10:1864.

Paglinawan R, Malipiero U, Schlapbach R, Frei K, Reith W, Fontana A. 2003. TGFbeta directs gene expression of activated microglia to an anti-inflammatory phenotype strongly focusing on chemokine genes and cell migratory genes. Glia 44:219–231.

Pandey RS, Graham L, Uyar A, Preuss C, Howell GR, Carter GW. 2019. Genetic perturbations of disease risk genes in mice capture transcriptomic signatures of late-onset Alzheimer's disease. Mol Neurodegener 14:50.

Pilotto A, Padovani A, Borroni B. 2013. Clinical, biological, and imaging features of monogenic Alzheimer's Disease. Biomed Res Int 2013:689591.

Podleśny-Drabiniok A, Marcora E, Goate AM. 2020. Microglial Phagocytosis: A Disease-Associated Process Emerging from Alzheimer's Disease Genetics. Trends in Neurosciences 43:965–979.

Pokatayev V, Hasin N, Chon H, Cerritelli SM, Sakhuja K, Ward JM, Morris HD, Yan N, Crouch RJ. 2016. RNase H2 catalytic core Aicardi-Goutières syndrome-related mutant invokes cGAS-STING innate immune-sensing pathway in mice. J Exp Med 213:329–336.

Prater KE, Aloi MS, Pathan JL, Winston CN, Chernoff RA, Davidson S, Sadgrove M, McDonough A, Zierath D, Su W, Weinstein JR, Garden GA. 2021. A Subpopulation of Microglia Generated in the Adult Mouse Brain Originates from Prominin-1-Expressing Progenitors. J Neurosci 41:7942–7953.

Prinz M, Jung S, Priller J. 2019. Microglia Biology: One Century of Evolving Concepts. Cell 179:292–311.

Qiu X, Mao Q, Tang Y, Wang L, Chawla R, Pliner HA, Trapnell C. 2017. Reversed graph embedding resolves complex single-cell trajectories. Nat Methods 14:979–982.

R Core Team. 2020. R: A language and environment for statistical computing. Vienna, Austria: R Foundation for Statistical Computing. Available from: https://www.R-project.org/

Rangaraju S, Dammer EB, Raza SA, Rathakrishnan P, Xiao H, Gao T, Duong DM, Pennington MW, Lah JJ, Seyfried NT, Levey AI. 2018. Identification and therapeutic modulation of a pro-inflammatory subset of disease-associated-microglia in Alzheimer's disease. Mol Neurodegener 13:24.

Reijns MAM, Rabe B, Rigby RE, Mill P, Astell KR, Lettice LA, Boyle S, Leitch A, Keighren M, Kilanowski F, Devenney PS, Sexton D, Grimes G, Holt IJ, Hill RE, Taylor MS, Lawson KA, Dorin JR, Jackson AP. 2012. Enzymatic removal of ribonucleotides from DNA is essential for mammalian genome integrity and development. Cell 149:1008–1022.

Rexach JE, Polioudakis D, Yin A, Swarup V, Chang TS, Nguyen T, Sarkar A, Chen L, Huang J, Lin L-C, Seeley W, Trojanowski JQ, Malhotra D, Geschwind DH. 2020. Tau Pathology Drives Dementia Risk-Associated Gene Networks toward Chronic Inflammatory States and Immunosuppression. Cell Reports 33:108398.

Riley JS, Tait SW. 2020. Mitochondrial DNA in inflammation and immunity. EMBO Rep 21:e49799.

van Rooij JGJ, Meeter LHH, Melhem S, Nijholt DAT, Wong TH, Rozemuller A, Uitterlinden AG, van Meurs JG, van Swieten JC. 2019. Hippocampal transcriptome profiling combined with protein-protein interaction analysis elucidates Alzheimer's disease pathways and genes. Neurobiology of Aging 74:225–233.

Roy ER, Wang B, Wan Y-W, Chiu G, Cole A, Yin Z, Propson NE, Xu Y, Jankowsky JL, Liu Z, Lee VM-Y, Trojanowski JQ, Ginsberg SD, Butovsky O, Zheng H, Cao W. 2020. Type I interferon response drives neuroinflammation and synapse loss in Alzheimer disease. J Clin Invest 130:1912–1930.

Saddala MS, Yang X, Tang S, Huang H. 2021. Transcriptome-wide analysis reveals core sets of transcriptional regulators of sensome and inflammation genes in retinal microglia. Genomics 113:3058–3071.

Sala Frigerio C, Wolfs L, Fattorelli N, Thrupp N, Voytyuk I, Schmidt I, Mancuso R, Chen W-T, Woodbury ME, Srivastava G, Möller T, Hudry E, Das S, Saido T, Karran E, Hyman B, Perry VH, Fiers M, De Strooper B. 2019. The Major Risk Factors for Alzheimer's Disease: Age, Sex, and Genes Modulate the Microglia Response to Aβ Plaques. Cell Rep 27:1293-1306.e6.

Salter MW, Stevens B. 2017. Microglia emerge as central players in brain disease. Nat Med 23:1018–1027.

Schoggins JW, Wilson SJ, Panis M, Murphy MY, Jones CT, Bieniasz P, Rice CM. 2011. A diverse array of gene products are effectors of the type I interferon antiviral response. Nature 472:481–485.

Shahidehpour RK, Higdon RE, Crawford NG, Neltner JH, Ighodaro ET, Patel E, Price D, Nelson PT, Bachstetter AD. 2021. Dystrophic microglia are associated with neurodegenerative disease and not healthy aging in the human brain. Neurobiology of Aging 99:19–27.

Sierksma A, Lu A, Mancuso R, Fattorelli N, Thrupp N, Salta E, Zoco J, Blum D, Buée L, De Strooper B, Fiers M. 2020. Novel Alzheimer risk genes determine the microglia response to amyloid-β but not to TAU pathology. EMBO Mol Med 12:e10606.

Sleegers K, Bettens K, De Roeck A, Van Cauwenberghe C, Cuyvers E, Verheijen J, Struyfs H, Van Dongen J, Vermeulen S, Engelborghs S, Vandenbulcke M, Vandenberghe R, De Deyn PP, Van Broeckhoven C, BELNEU consortium. 2015. A 22-single nucleotide polymorphism Alzheimer's disease risk score correlates with family history, onset age, and cerebrospinal fluid Aβ42. Alzheimers Dement 11:1452–1460.

Small SA, Kent K, Pierce A, Leung C, Kang MS, Okada H, Honig L, Vonsattel J-P, Kim T-W. 2005. Model-guided microarray implicates the retromer complex in Alzheimer's disease. Ann Neurol 58:909–919.

Smolders SM-T, Kessels S, Vangansewinkel T, Rigo J-M, Legendre P, Brône B. 2019. Microglia: Brain cells on the move. Progress in Neurobiology 178:101612.

Song X, Aw JTM, Ma F, Cheung MF, Leung D, Herrup K. 2021. DNA repair inhibition leads to active export of repetitive sequences to the cytoplasm triggering an inflammatory response. J Neurosci:JN-RM-0845-21.

Song X, Ma F, Herrup K. 2019. Accumulation of Cytoplasmic DNA Due to ATM Deficiency Activates the Microglial Viral Response System with Neurotoxic Consequences. J Neurosci 39:6378–6394.

Sørensen DM, Holemans T, van Veen S, Martin S, Arslan T, Haagendahl IW, Holen HW, Hamouda NN, Eggermont J, Palmgren M, Vangheluwe P. 2018. Parkinson disease related ATP13A2 evolved early in animal evolution. PLoS One 13:e0193228.

Spittau B, Dokalis N, Prinz M. 2020. The Role of TGFβ Signaling in Microglia Maturation and Activation. Trends in Immunology 41:836–848.

Srinivasan K, Friedman BA, Etxeberria A, Huntley MA, van der Brug MP, Foreman O, Paw JS, Modrusan Z, Beach TG, Serrano GE, Hansen DV. 2020. Alzheimer's Patient Microglia Exhibit Enhanced Aging and Unique Transcriptional Activation. Cell Reports 31:107843.

Stancu I-C, Cremers N, Vanrusselt H, Couturier J, Vanoosthuyse A, Kessels S, Lodder C, Brône B, Huaux F, Octave J-N, Terwel D, Dewachter I. 2019. Aggregated Tau activates NLRP3-ASC inflammasome exacerbating exogenously seeded and non-exogenously seeded Tau pathology in vivo. Acta Neuropathol 137:599–617.

Street K, Risso D, Fletcher RB, Das D, Ngai J, Yosef N, Purdom E, Dudoit S. 2018. Slingshot: cell lineage and pseudotime inference for single-cell transcriptomics. BMC Genomics 19:477.

Streit WJ, Braak H, Xue Q-S, Bechmann I. 2009. Dystrophic (senescent) rather than activated microglial cells are associated with tau pathology and likely precede neurodegeneration in Alzheimer's disease. Acta Neuropathol 118:475–485.

Streit WJ, Khoshbouei H, Bechmann I. 2020. Dystrophic microglia in late-onset Alzheimer's disease. Glia 68:845–854.

Streit WJ, Sammons NW, Kuhns AJ, Sparks DL. 2004. Dystrophic microglia in the aging human brain. Glia 45:208–212.

Streit WJ, Xue Q-S, Tischer J, Bechmann I. 2014. Microglial pathology. Acta Neuropathol Commun [Internet] 2. Available from: https://www.ncbi.nlm.nih.gov/pmc/articles/PMC4180960/

Stuart T, Butler A, Hoffman P, Hafemeister C, Papalexi E, Mauck WM, Hao Y, Stoeckius M, Smibert P, Satija R. 2019. Comprehensive integration of single-cell data. Cell 177:1888-1902.e21.

Subramanian N, Natarajan K, Clatworthy MR, Wang Z, Germain RN. 2013. The adapter MAVS promotes NLRP3 mitochondrial localization and inflammasome activation. Cell 153:348–361.

Swanson KV, Deng M, Ting JP-Y. 2019. The NLRP3 inflammasome: molecular activation and regulation to therapeutics. Nat Rev Immunol 19:477–489.

Tay TL, Mai D, Dautzenberg J, Fernandez-Klett F, Lin G, Sagar, Datta M, Drougard A, Stempfl T, Ardura-Fabregat A, Staszewski O, Margineanu A, Sporbert A, Steinmetz LM, Pospisilik JA, Jung S, Priller J, Grun D, Ronneberger O, Prinz M. 2017. A new fate mapping system reveals context-dependent random or clonal expansion of microglia. Nat Neurosci 20:793–803.

Thrupp N, Sala Frigerio C, Wolfs L, Skene NG, Fattorelli N, Poovathingal S, Fourne Y, Matthews PM, Theys T, Mancuso R, de Strooper B, Fiers M. 2020. Single-Nucleus RNA-Seq Is Not Suitable for Detection of Microglial Activation Genes in Humans. Cell Reports 32:108189.

Thurman AL, Ratcliff JA, Chimenti MS, Pezzulo AA. 2021. Differential gene expression analysis for multi-subject single-cell RNA-sequencing studies with aggregateBioVar. Bioinformatics 37:3243–3251.

Toro H, Hidalgo H, Cardoso W, Morales MA. 1990. Screening for antibodies against infectious bronchitis virus: specificity of the haemagglutination inhibition test. Zentralbl Veterinarmed B 37:254–256.

Trapnell C, Cacchiarelli D, Grimsby J, Pokharel P, Li S, Morse M, Lennon NJ, Livak KJ, Mikkelsen TS, Rinn JL. 2014. Pseudo-temporal ordering of individual cells reveals dynamics and regulators of cell fate decisions. Nat Biotechnol 32:381–386.

Ulland TK, Song WM, Huang SC-C, Ulrich JD, Sergushichev A, Beatty WL, Loboda AA, Zhou Y, Cairns NJ, Kambal A, Loginicheva E, Gilfillan S, Cella M, Virgin HW, Unanue ER, Wang Y, Artyomov MN, Holtzman DM, Colonna M. 2017. TREM2 maintains microglial metabolic fitness in Alzheimer's disease. Cell 170:649-663.e13.

Van Acker ZP, Bretou M, Annaert W. 2019. Endo-lysosomal dysregulations and late-onset Alzheimer's disease: impact of genetic risk factors. Mol Neurodegener 14:20.

Van Acker ZP, Perdok A, Bretou M, Annaert W. 2021. The microglial lysosomal system in Alzheimer's disease: Guardian against proteinopathy. Ageing Res Rev 71:101444.

Van Damme P, Robberecht W. 2021. STING-Induced Inflammation — A Novel Therapeutic Target in ALS? | NEJM. New England Journal of Medicine [Internet]. Available from: https://www-nejm-org.offcampus.lib.washington.edu/doi/10.1056/NEJMcibr2031048

Voet S, Srinivasan S, Lamkanfi M, van Loo G. 2019. Inflammasomes in neuroinflammatory and neurodegenerative diseases. EMBO Mol Med [Internet] 11. Available from: https://www.ncbi.nlm.nih.gov/pmc/articles/PMC6554670/

Wang D, Zhang J, Jiang W, Cao Z, Zhao F, Cai T, Aschner M, Luo W. 2017. The role of NLRP3-CASP1 in inflammasome-mediated neuroinflammation and autophagy dysfunction in manganese-induced, hippocampal-dependent impairment of learning and memory ability. Autophagy 13:914–927.

Wang F, Gómez-Sintes R, Boya P. 2018. Lysosomal membrane permeabilization and cell death. Traffic 19:918–931.

Warburg O, Wind F, Negelein E. 1927. THE METABOLISM OF TUMORS IN THE BODY. J Gen Physiol 8:519–530.

Webers A, Heneka MT, Gleeson PA. 2020. The role of innate immune responses and neuroinflammation in amyloid accumulation and progression of Alzheimer's disease. Immunology & Cell Biology 98:28–41.

Wenzel J, Ouderkirk JL, Krendel M, Lang R. 2015. The class I myosin Myo1e regulates TLR4-triggered macrophage spreading, chemokine release and antigen presentation via MHC class II. Eur J Immunol 45:225–237.

Wickham H, Chang W, Henry L, Pedersen TL, Takahashi K, Wilke C, Woo K, Yutani H, Dunnington D. 2016. ggplot2: Elegant Graphics for Data Analysis. Springer-Verlag New York. Available from: https://ggplot2.tidyverse.org

Wolf SA, Boddeke HWGM, Kettenmann H. 2017. Microglia in Physiology and Disease. Annu Rev Physiol 79:619–643.

Wolock SL, Lopez R, Klein AM. 2019. Scrublet: Computational Identification of Cell Doublets in Single-Cell Transcriptomic Data. Cell Syst 8:281-291.e9.

Wu L, Rosa-Neto P, Hsiung G-YR, Sadovnick AD, Masellis M, Black SE, Jia J, Gauthier S. 2012. Early-onset familial Alzheimer's disease (EOFAD). Can J Neurol Sci 39:436–445.

Wu T, Hu E, Xu S, Chen M, Guo P, Dai Z, Feng T, Zhou L, Tang W, Zhan L, Fu X, Liu S, Bo X, Yu G. 2021. clusterProfiler 4.0: A universal enrichment tool for interpreting omics data. Innovation [Internet] 2. Available from: https://www.cell.com/the-innovation/abstract/S2666-6758(21)00066-7

Ye B, Yang G, Li Y, Zhang C, Wang Q, Yu G. 2020. ZNF143 in Chromatin Looping and Gene Regulation. Front Genet 11:338.

Young JE, Fong LK, Frankowski H, Petsko GA, Small SA, Goldstein LSB. 2018. Stabilizing the Retromer Complex in a Human Stem Cell Model of Alzheimer's Disease Reduces TAU Phosphorylation Independently of Amyloid Precursor Protein. Stem Cell Reports 10:1046–1058.

Young MD, Behjati S. 2020. SoupX removes ambient RNA contamination from droplet-based single-cell RNA sequencing data. Gigascience 9:giaa151.

Yu G, Wang L-G, Han Y, He Q-Y. 2012. clusterProfiler: an R Package for Comparing Biological Themes Among Gene Clusters. OMICS: A Journal of Integrative Biology 16:284–287.

Zhou Y, Song WM, Andhey PS, Swain A, Levy T, Miller KR, Poliani PL, Cominelli M, Grover S, Gilfillan S, Cella M, Ulland TK, Zaitsev K, Miyashita A, Ikeuchi T, Sainouchi M, Kakita A, Bennett DA, Schneider JA, Nichols MR, Beausoleil SA, Ulrich J, Holtzman DM, Artyomov MN, Colonna M. 2020. Human and mouse single-nucleus transcriptomics reveal TREM2-dependent and -independent cellular responses in Alzheimer's disease. Nat Med 26:131–142.

Table 1. Post-mortem brain sample demographics.

Group	Males	Females	Avg. Age	Avg. PMI	ADNC	E2/3	E3/3	E3/4	E4/4
Ctrl	4	6	85.9	5.53	0-1	2	7	1	
AD	3	9	86.5	4.67	2-3		6	5	1
Total	7	15	86.23	5.42		2	13	6	1

Ctrl = Control, AD = Alzheimer's Disease pathology, PMI = post-mortem interval, ADNC = Alzheimer's Disease Neuropathic Change, APOE Genotypes: APOE alleles 2/3 (E2/3) , APOE alleles 3/3 (E3/3) , APOE alleles 3/4 (E3/4), APOE alleles 4/4 (E4/4)

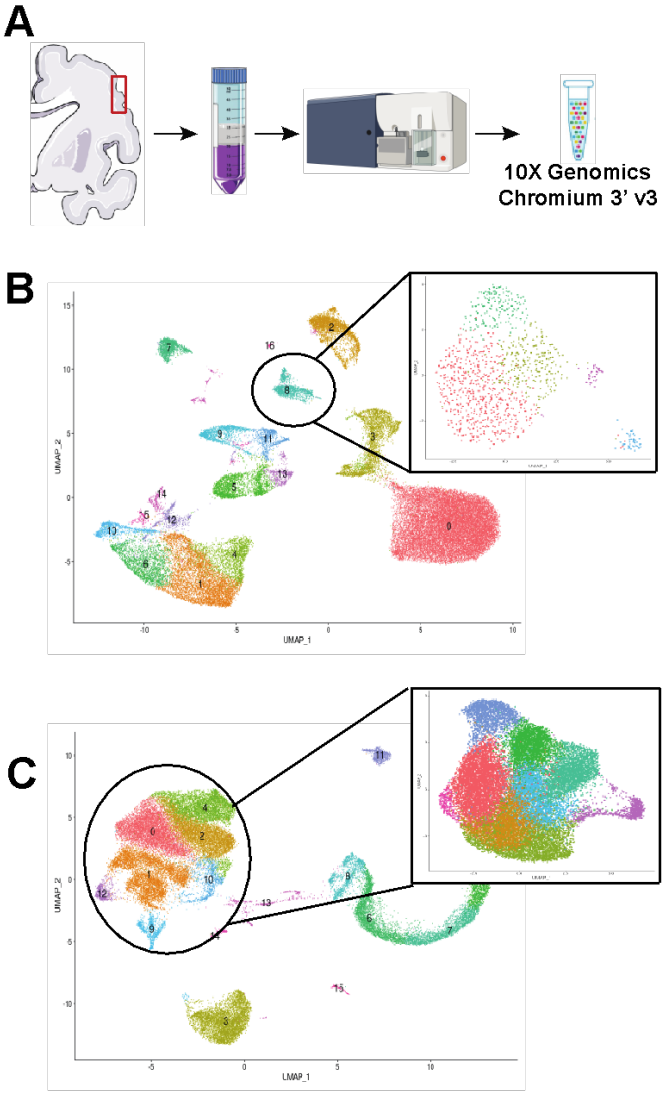

Figure 1. PU.1 enrichment increases the number of microglia nuclei and enhances microglia subpopulation resolution in snRNAseq studies. A) Nuclei isolated from dorsolateral prefrontal cortex grey matter of postmortem human brain tissue sorted by fluorescence-activated nuclei sorting using the myeloid marker PU.1 and then sequenced on the 10X Genomics Chromium 3' v3 platform. **B)** Unsorted snRNAseq data from four samples demonstrates multiple

brain cell types and a small population of microglia (1032) that can be further subdivided into five subpopulations. **C)** After PU.1 enrichment, an snRNAseq dataset from the same four individuals contains a large number of microglia (23310), and these microglia can be further subclustered into nine subpopulations.

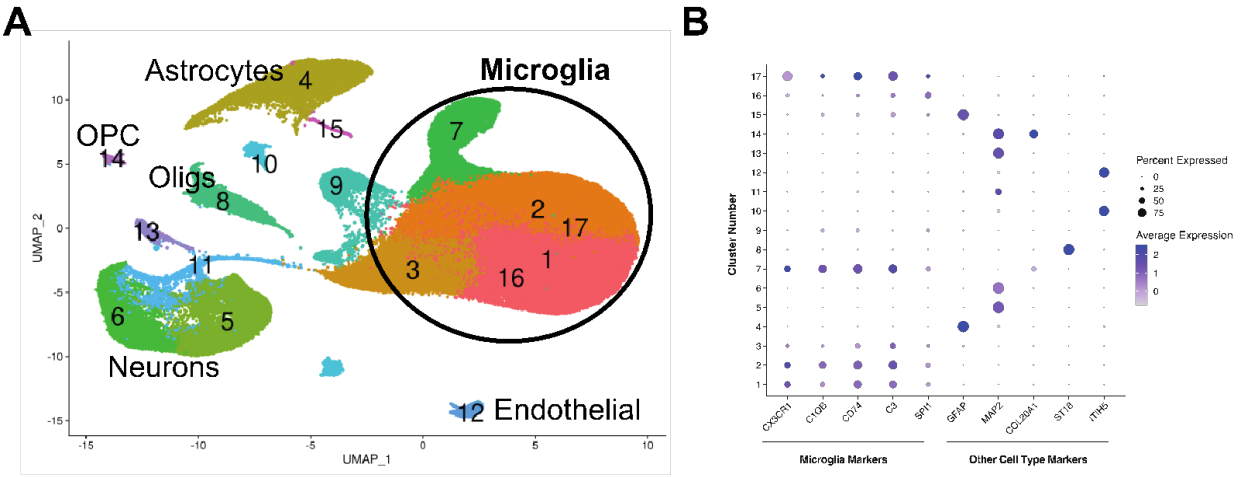

Figure 2. PU.1 enrichment provides increased numbers of microglia nuclei. A) UMAP of all nuclei in the 22 subject dataset demonstrates that while other cell types including neurons, astrocytes, oligodendrocytes (Oligs) and their progenitors (OPC) as well as endothelial cells are present, six clusters including the three largest are composed of microglia nuclei. **B)** Representative cell type marker genes (x-axis) with the percent of nuclei that express a gene (size of dot) in each cluster (distributed along Y axis) and the average expression level (color intensity) are shown for microglia (*CX3CR1, C1QB, CD74*, and *C3*), astrocytes (*GFAP*), neurons (*MAP2*), OPCs (*COL20A1*), oligodendrocytes (*ST18*), and endothelial cells (*ITIH5*) for each cluster.

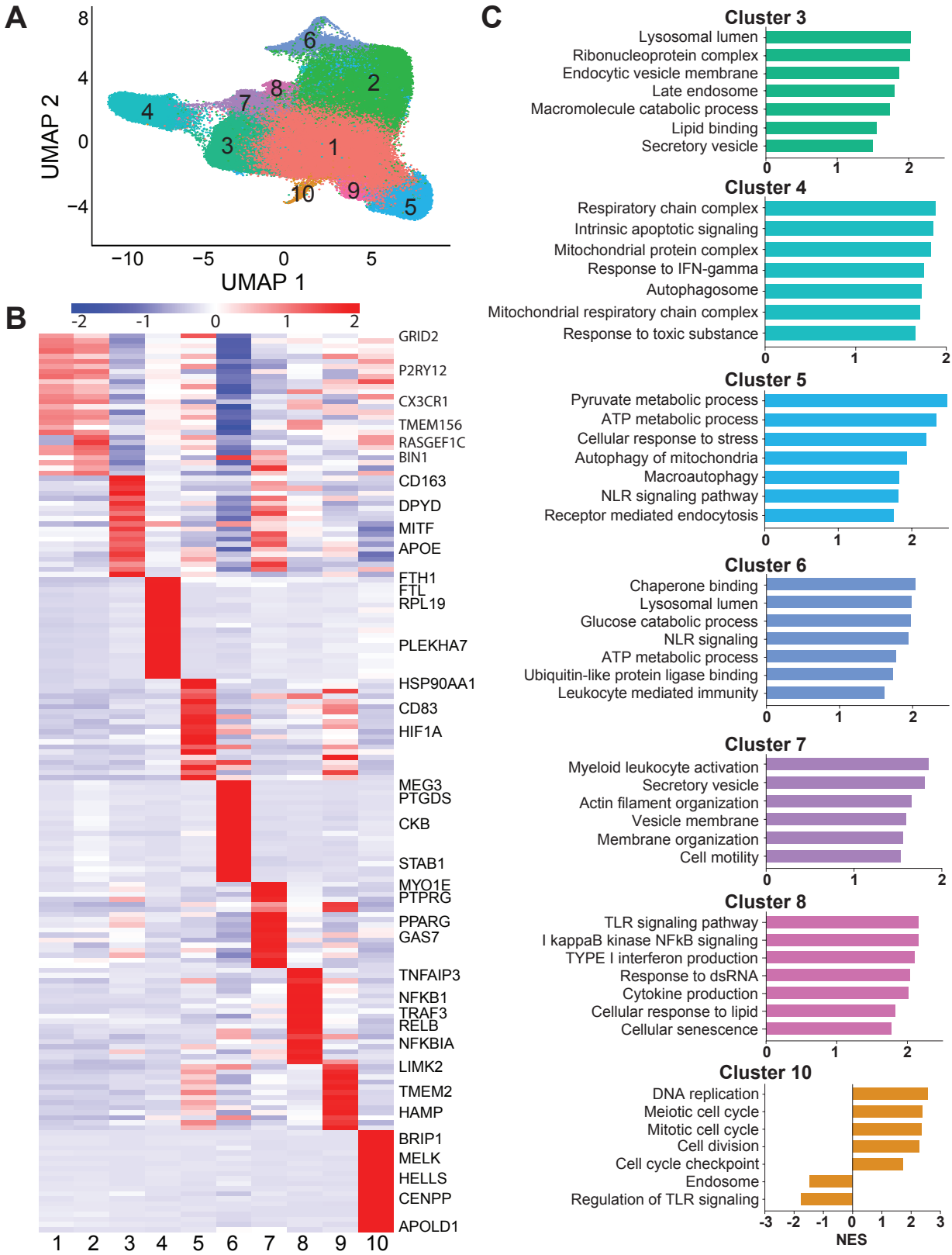

Figure 3. Microglia subpopulations reveal a wide diversity of gene expression and biological pathway correlates. A) UMAP of unbiased clustering on the mixed APOE genotype

22 sample dataset contains 10 microglia subpopulations. **B)** Differential expression analysis comparing each cluster to all other clusters demonstrates distinct gene expression profiles for each. The top 25 genes from each cluster are displayed in the heatmap, with gene names of particular biological interest annotated on the right. Cluster 1 is high in canonical microglia genes (*CX3CR1* and *P2RY12*) thought to be highly expressed in an unactivated state, so we label this cluster "homeostatic". **C)** GSEA analysis of genes that differentiate each cluster from cluster 1 ("homeostatic") suggest distinct biological pathways and function correlates for each cluster. Pathways displayed are GO, but are representative of pathways that were significantly altered in two of KEGG, Reactome, and GO databases.

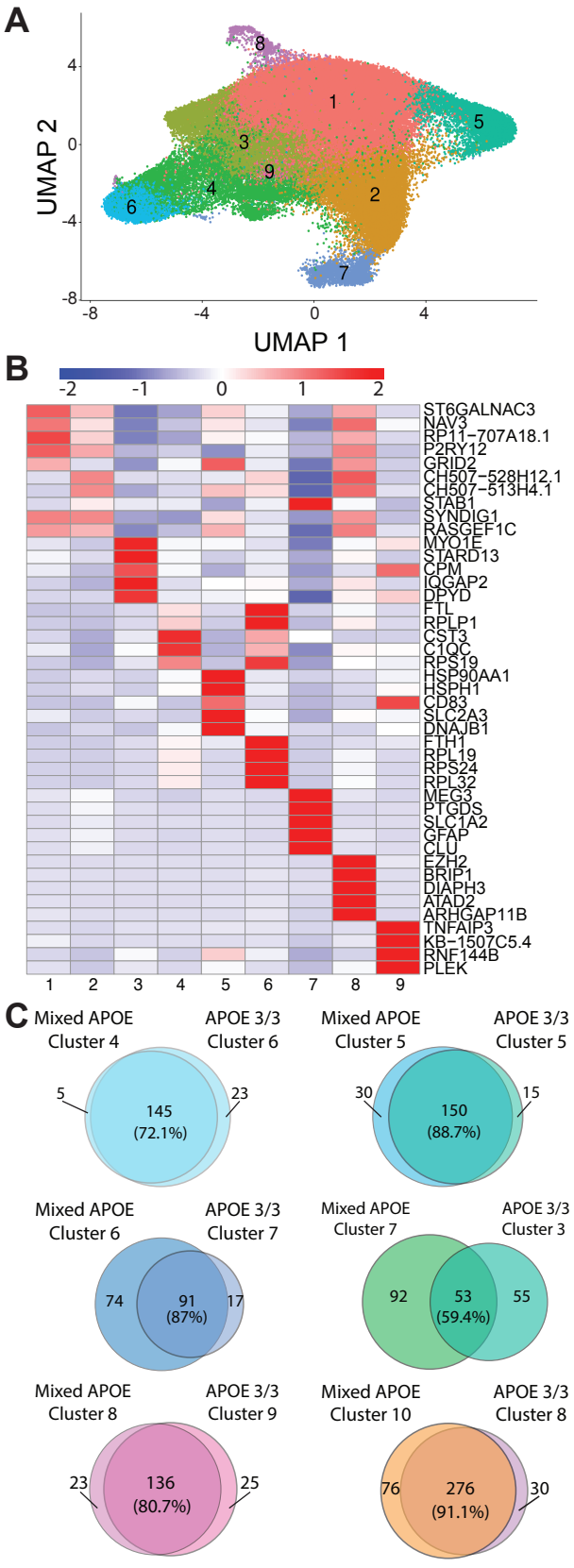

Figure 4. APOE 3/3 genotype does not substantially alter microglial clustering in human autopsy brain. A) UMAP of unbiased clustering on 13 samples of only APOE 3/3 individuals shows 9 clusters. **B)** Similar to the clusters identified in the mixed APOE genotype dataset, the clusters identified in our APOE 3/3 genotype dataset are highly distinct by gene expression. The top 5 genes are displayed for each cluster. **C)** Venn diagrams demonstrating overlap between clusters from the Mixed APOE and APOE 3/3 cohorts demonstrating significant similarity in gene expression profiles.

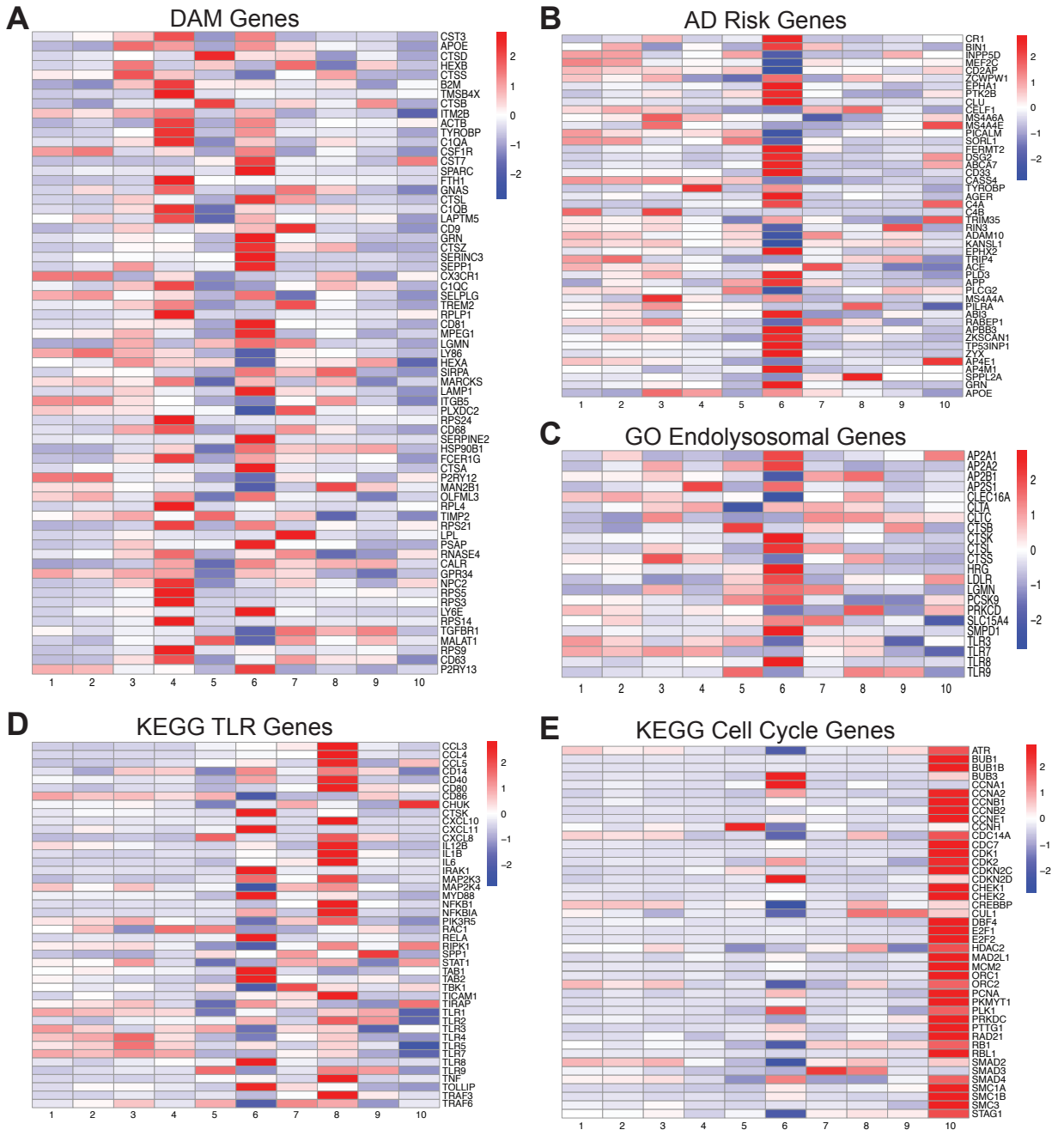

Figure 5. Previously defined gene lists demonstrate unique expression in microglia subpopulations, including AD risk genes specifically enriched in cluster 6. A) DAM genes as defined by Keren-Shaul et al. (2017) were statistically enriched in cluster 4 using GSEA analysis, and the heatmap demonstrates upregulation of many of these genes. Cluster 6 also demonstrates upregulation of some DAM genes, distinct from those in cluster 4. **B)** Genes associated with AD risk SNPs are highly enriched in cluster 6. **C)** Heatmap of genes from the GO endolysosomal pathway geneset demonstrating significant enrichment in cluster 6, cluster 3, 5, and 7. **D)** Heatmap of representative genes from the KEGG toll-like receptor pathway geneset illustrating significant enrichment in cluster 8, of many genes (Supplemental data) as would be

expected given the inflammatory phenotype. **E)** Gene expression of representative genes from the KEGG cell cycle pathway geneset demonstrates significant enrichment in cluster 10.

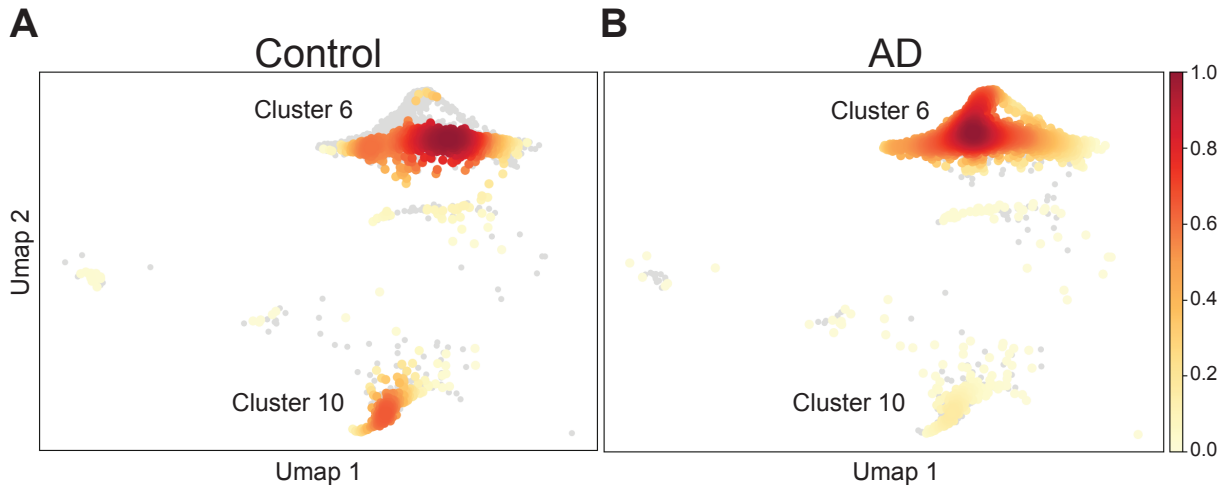

Figure 6. Cluster 6 is larger and cluster 10 is depleted in AD brain. Normalized density of nuclei is displayed by color; dark red is the highest nuclei density region on the UMAP, yellow the least dense collection of nuclei. Grey dots indicate nuclei from the opposite group (i.e. grey dots in controls indicate nuclei that are from AD individuals). **A)** Density of nuclei in cluster 6 and cluster 10 in control individuals compared to **B)** density of nuclei in cluster 6 and cluster 10 in AD individuals. Cluster 6 is more highly represented by AD nuclei, while cluster 10 shows higher representation of controls.

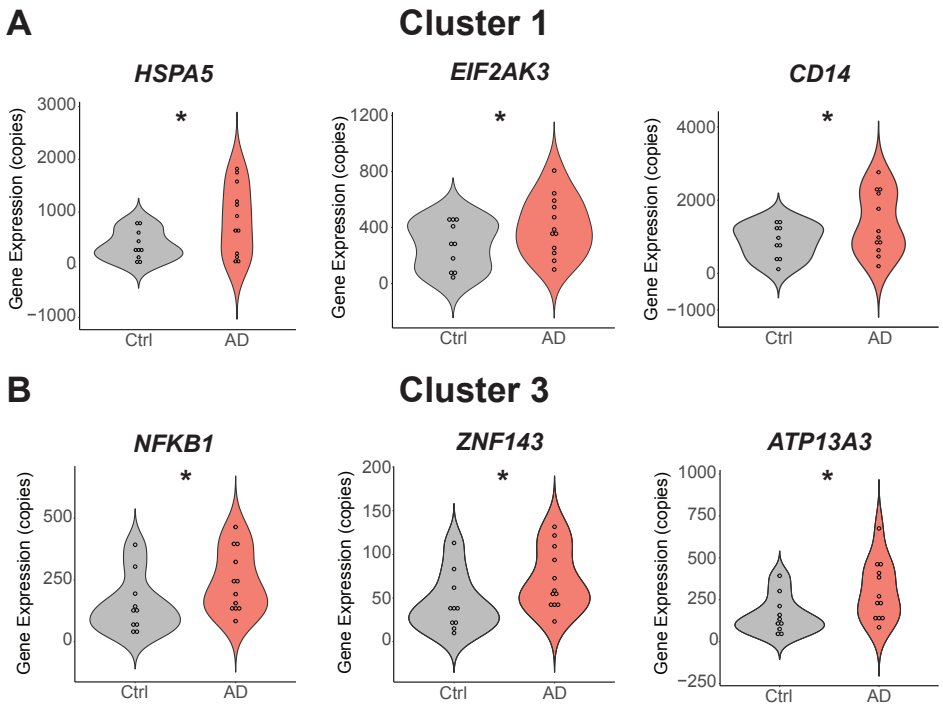

Figure 7. Unactivated microglia subpopulations show upregulation of inflammatory and stress-related gene expression in AD brain. A) Cluster 1 genes that were significantly upregulated in AD brain compared to Controls included *HSPA5* (q = 0.056), *EIF2AK3* (q = 0. 083), and *CD14* (q = 0. 055) genes involved in inflammation and endoplasmic reticulum stress processes. **B)** Cluster 3 genes that were significantly upregulated in AD brain compared to Controls include *NFKB1* (q = 0. 052), *ZNF143* (q = 0. 084), and *ATP13A3* (q = 0. 078) involved in NFκB signaling, response to DNA damage and recycling endosomes. Pro-inflammatory changes were not identified in more activated clusters, cluster 6 and cluster 8, suggesting that these are subpopulation-specific effects.